Volume 1 *December 1931* *Number 6*

PHYSICS

SOME EXPERIMENTS WITH GAS-FILLED Cs–O–Ag PHOTO CELLS

By K. H. Kingdon and H. E. Thomson[1]

Research Laboratories, General Electric Company

(Received November 2, 1931)

Abstract

The *amplification* of the cathode emission *by argon* is much greater for a tube with a photo-cathode, than for a tube of similar geometry equipped with a thermionic cathode. This difference is attributed to large *secondary electron emission* by positive ion bombardment of the photo-cathode. If the *anode voltage* of one of these argon-filled tubes is *abruptly increased*, the *time lag* in the resulting current change is of the order 5×10^{-5} sec. for the thermionic tube, but of the order 10^{-3} sec. for the photo-tube. This lag is attributed to the life of the positive ion charge on the spongy surface of the photo-cathode. Measurements of the *spontaneous fluctuations* in the current through a gas-filled photo-tube indicate that the "noise" is of low frequency and associated with the gas amplification effect.

IT HAS been found that if a silver surface is first oxidized in an electrical discharge, and then baked in the presence of caesium vapor, it may be converted into a photo-cathode of remarkable sensitivity.[2] A good cathode of this type will give in vacuum a photoemission of about 10^{-5} amp. per lumen (incandescent lamp at 2870°K), and this yield may be increased 5 or 10-fold by filling the cell with argon at a pressure of 0.1 mm. It appears that the underlying layers of the cathode consist of Cs_2O, formed by reduction of the oxidized silver, and perhaps containing some free silver as an aid to electrical conduction. The outermost layer of the cathode probably consists of adsorbed Cs atoms which are held by the base layers in such spacing as to give the optimum low work function. Thermionic measurements[3] with films of caesium and oxygen on tungsten have shown that definite surface densities of both oxygen and caesium atoms are necessary to give the lowest work function, and Becker[4] has shown that this optimum concentration of Cs atoms is 4.1×10^{14} per cm². It may be significant that the density[5] of Cs_2O is 4.36 gm/cm³, which corresponds to 4.4×10^{14} molecules per cm² of surface, so that an adsorption on the surface of one Cs atom per Cs_2O molecule would give a

[1] These experiments were done towards the end of 1929.

[2] K. Bainbridge and E. E. Charlton, Unpublished work in this laboratory.
L. R. Koller, G. E. Review **31**, 476 (1928); Phys. Rev. **33**, 1082 (1929).
N. R. Campbell, Photoelectric Symposium, Phys. Soc. of London, June 4 (1930); Phil. Mag. **12**, 173 (1931).

[3] I. Langmuir and K. H. Kingdon, Proc. Roy. Soc. **A107**, 61 (1925).

[4] J. A. Becker, Phys. Rev. **28**, 341 (1926).

[5] Int. Critical Tables, Vol. 1, page 160.

surface density of caesium about equal to that found to be best in the thermionic measurements.

It is evident that delicate adjustment of the amounts of oxygen and caesium in the cell is necessary in order to finish up with the optimum surface layer of caesium: too much, or too little caesium makes the cathode insensitive. Moreover the sensitive surface is of course readily attacked by water-vapor or oxygen, and it is remarkable that the surface layer in these cells is not appreciably changed by residual gas impurities during a life period of hundreds of hours. This must be due to an extraordinarily thorough clean-up of such gases in the glass walls and electrodes by the hot caesium vapor during the baking process.

Fig. 1 shows the type of tube used in these experiments. *C* is the photo-cathode, *A* the anode, and *P* the pellet containing the caesium compound from which the caesium is made by high frequency induction heating.

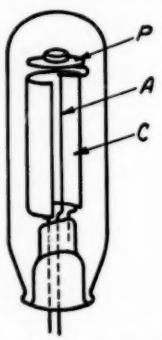

Fig. 1 Construction of photo-cell.

The Rôle of Argon in Amplifying Photo-Currents

It has been suggested that a large part of the increase in photo-current produced by filling the cell with argon is probably secondary electron emission caused by the impact of positive ions on the cathode. The following experiments were made to obtain more information about this secondary current due to the gas.

Two types of tubes were constructed shown in cross-section in Fig. 2, *A* and *B*. Both types had exactly similar bulbs. *A* was the standard type (Fig. 1) Cs–O–Ag photo-cell, with semi-cylindrical cathode *c*, and wire anode

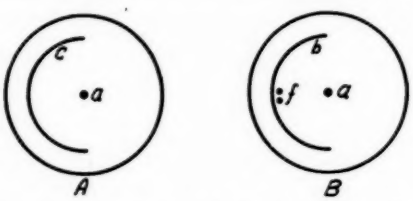

Fig. 2. Cross-sections of photo (*A*) and thermionic (*B*) tubes.

a. Type *B* had the same kind of anode, and was also equipped with a semi-cylinder of nickel *b* of the same size and shape as the photo-cathode *c*. About 1 mm in front of *b* was mounted a small tungsten loop filament *f*; the tip of

this filament was connected to *b*. Both types of tubes were filled with argon to various pressures.

Fig. 3 shows typical volt-ampere characteristics obtained with tubes of the two types. The full curves show data taken with a thermionic (type *B*) tube, containing argon at 0.2 mm pressure, and at the various filament heating currents marked on the curves. At the lowest filament temperatures the thermionic emission saturates fairly well at low voltages, while at the higher voltages the curves show a rise due to ionization. At the higher filament temperatures the saturation and ionization parts of the curves merge into one another. At lower pressures the thermionic tube shows proportionally less gas amplification. The dotted curve shows data taken with a photo-cell (type *A*) containing argon at 0.123 mm pressure. The curve shows a

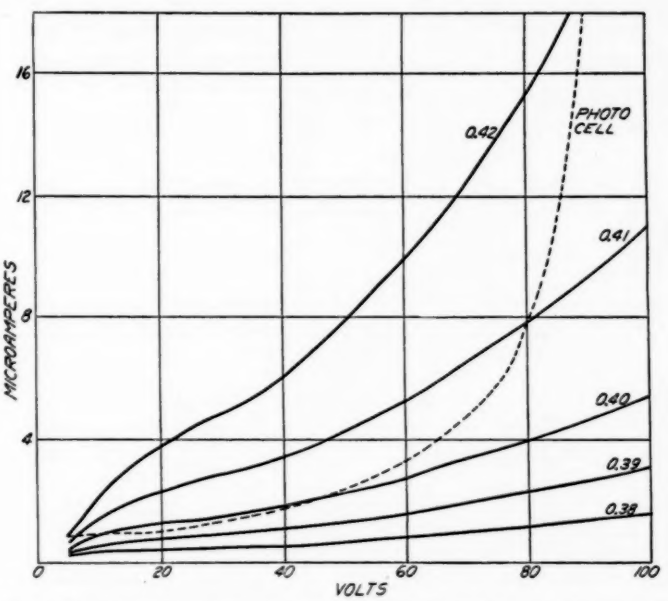

Fig. 3. Current-voltage characteristics of thermionic and photo-tubes.

primary photo-current of about 1 microampere, which is amplified by the gas effects at higher voltages to a much greater extent than is the case in the thermionic tube—in spite of the adverse pressure difference between the two tubes. Both tubes offer equal path lengths and potential distributions for ionization by collision effects, so that the difference in their behavior must be due to some other cause, such as the emission of secondary electrons from the photo-cathode by positive ion bombardment.

It should be mentioned that in vacuum cells of both types, primary thermionic or photoelectric currents of the order 1 microampere showed no important increase as the anode voltage was changed from 20 to 120. Poor saturation is therefore not the cause of the difference in the gas-filled tubes.

We also made experiments in which a photo-cathode was surrounded by a grid, and argon light produced by the current flow from a second cathode in

the same bulb fell on the first cathode. The grid was used in the Davis and Goucher[6] manner to determine whether current to the first cathode was due to collection of ions or to emission of photoelectrons. It appeared that no considerable current could be ascribed to the action of the argon radiation. Hence photoeffect of radiation is not responsible for the difference in the behavior of tubes of types *A* and *B* above.

Experiments on Time Lag

Experiments were also made with tubes of types *A* and *B* to study time-lag effects associated with the establishment of the gas-amplified currents at the higher anode voltages. In these experiments the anode voltage of the tube was abruptly changed from a low value (sufficient to saturate the primary emission) to a higher value (sufficient to give a considerable gas amplification effect), and the manner in which the anode current changed with time was observed with a cathode-ray oscillograph. The electrical circuit used to do this is shown in Fig. 4. A simple commutator made and broke a circuit at *L* about 400 times per second. It will be clear from the diagram that when

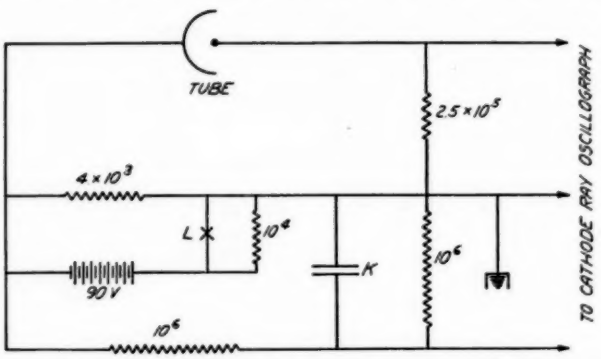

Fig. 4. Circuit for studying time-lags in tube current accompanying change of tube voltage.

this break was closed, the full battery voltage (90) appeared across the tube (except for the drop in the 250,000 ohm load resistance). When the break was open, the voltage across the tube was reduced to

$$90 \times \frac{4000}{10{,}000 + 4000} = 26 \text{ volts.}$$

The timing wave for the cathode-ray oscillograph was obtained from the charging of condenser *K*. For the observations to which we wish to refer this condenser was 4×10^{-10} farad, and the time constant for its rate of charging was 2×10^{-4} second.

The capacity of the tube and connections to the cathode-ray oscillograph were kept as small as possible—usually about 10^{-11} farad. The oscillograph patterns were traced by hand on pieces of tracing cloth, so that the accuracy of the tracings was rather poor.

[6] Davis and Goucher, Phys. Rev. **10**, 101 (1917).

Fig. 5 shows a curve obtained with a thermionic tube (B) containing argon at 0.2 mm. The logarithmic time scale of the tracing has been made linear and the time axis made continuously progressive. The base line of

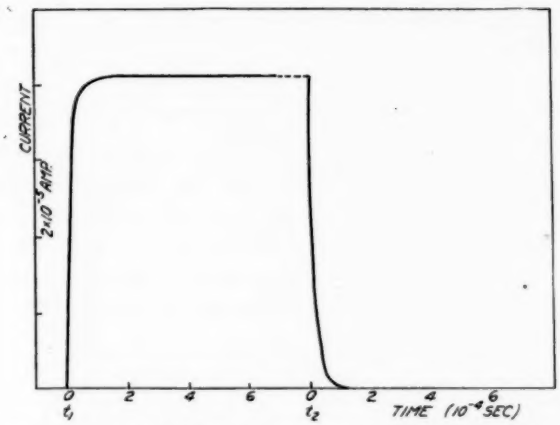

Fig. 5. Changes in thermionic tube current when anode voltage is changed from 26 to 90 and back again.

Fig. 5 does not represent zero current through the cell, but rather the primary thermionic current at an anode voltage of 26. The anode voltage was raised to 90 at the instant t_1, and the current had almost reached its final amplified value 5×10^{-5} sec. later. At the instant t_2 the voltage was lowered to 26, and the current fell to its base value in a little more than 5×10^{-5} sec. These time lags may be satisfactorily explained as the times required for the establishment and sweeping out, respectively, of the ionization in the tube.

Fig. 6 shows the tracing obtained when a photo-cell (A) containing 0.2 mm argon was subjected to the same voltage cycle. The light intensity was adjusted to give about the same maximum current as in Fig. 5. The base line

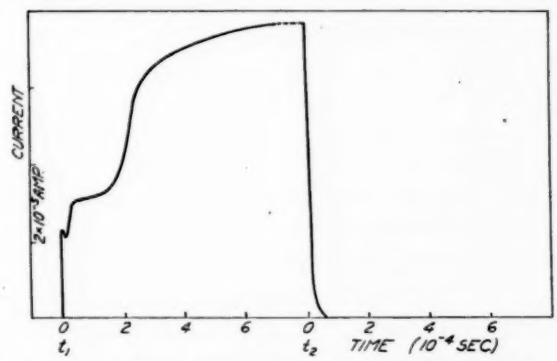

Fig. 6. Changes in photo-tube current when anode voltage is changed from 26 to 90 and back again.

again represents the primary photoelectric current at a voltage of 26. When the voltage was changed abruptly to 90 at time t_1, there occurred first a slight capacity current kick. The current then built up to a quasi-saturation value

in about 5×10^{-5} sec. This is presumably the same ionization phenomenon as occurred in the thermionic tube. In the photoelectric tube there was, however, a further increase of current which continued up to about 0.001 sec.; that is, to the end of the half-cycle. This delayed current rise was presumably caused by the factor which makes the gas amplification in a photo-cell greater than in a similar thermionic tube. When the anode voltage was reduced to 26 at time t_2, the photo-current fell to its base value in about 5×10^{-5} sec.

If the voltage on the photo-tube is held constant at a value sufficient to give large ionization and the light is "chopped," current-time curves of the kind shown in Fig. 7 have been obtained by Metcalf,[7] by Campbell and Stoodley,[8] and by others. We also have observed this phenomenon. Here the lag occurs both when the light is admitted and when it is cut off. The period of the lag may be of the same order as that which we observed in the "voltage-chopping" experiments.

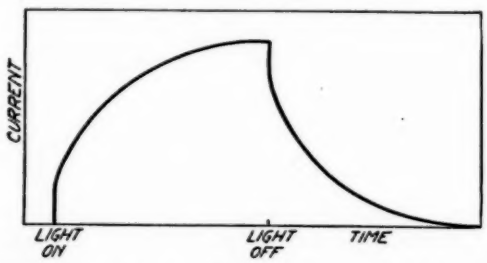

Fig. 7. Changes in photo-tube current when light is "chopped" and anode voltage held constant.

It seems to us that the explanation of these lag effects is as follows. The photo-cathode has rather a spongy surface which presumably is not of the highest electrical conductivity. When a positive ion strikes the surface, it delivers its kinetic and potential (recombination) energy to the surface, and this energy heats a small patch of the surface. If the surface is a poor electrical conductor, an appreciable time (10^{-3} sec.?) will be required for electrons to flow in to completely neutralize this positive charge. The excess thermal energy may be dissipated somewhat more quickly, for in poor conductors the ratio of thermal to electrical conduction is greater than in good conductors. Thus each positive ion as it strikes the surface produces a transient heating of the surface, and a somewhat longer-lived positive charging of the surface. This positive charge produces a field at the surface of the cathode, which effectively reduces the work-function in the manner described by Schottky.

A small decrease in work-function produced in this way will increase the secondary emission due to positive ion bombardment much more than it will affect the photo-emission. The secondary emission is probably thermionic current from spots on the cathode heated by positive ion bombardment.[9] If this is so, a small change in the work-function of the cathode will make a

[7] G. F. Metcalf, Unpublished work in this laboratory.
[8] Campbell and Stoodley, Symposium on Photoelectricity, Phys. Soc. London, June (1930).
[9] P. L. Kapitza, Phil. Mag. **45**, 989 (1923).

pronounced change in the secondary emission. On the other hand, most of the photoelectrons emitted from a thin-film cathode have energies near the maximum possible energy which may be obtained from the light,[10] so that there is no large number of low-velocity electrons which may be allowed to escape by a small reduction in work function. Accordingly, in the "chopped voltage" curve the extra current largely disappears as soon as the voltage is reduced and the ion bombardment stops; whereas in the chopped light curves, when the light is cut off and the voltage remains, the positive ion bombardment and secondary emission do not decrease abruptly (5×10^{-5} sec.), but die away at a rate determined by the decay of the positive charge on the surface of the cathode.

It was thought at first that the impacting ions might change the cathode surface mechanically in such a way as to make it a better secondary emitter, and that the time-lag was connected with the life of this mechanical change. This view appears quantitatively impossible, for the average positive ion current in Fig. 6 cannot be much greater than 10^{-5} amp., so that during any one voltage cycle not more than 10^{11} positive ions can strike the cathode, and it is inconceivable that this number of ions should produce an appreciable mechanical change in a surface containing 10^{15} atoms.

The idea that these 10^{11} ions produce by their electrical charge a change in the work function is better quantitatively, for if we say that half of their positive charge is still present at the end of the high voltage half-cycle, this would mean a charge density per cm² of about 5 e.s.u., and therefore an average electric field near the surface of 18000 volt/cm. On the Schottky theory this would correspond to a reduction in work function of 0.05 volt, or a decrease in the thermionic b of about 600 degrees. If the secondary electrons arise from thermionic emission from spots heated by the impact of ions, we may use Koller's data[11] for the thermionic emission from similar photocathodes to estimate whether our theory is possible quantitatively. His formula for the thermionic emission is

$$i = 0.098T^2e^{-8700/T} \text{ amp./cm}^2,$$

from which we find 0.0186 amp./cm² at 600°K. If b is reduced from 8700 to 8100 the emission will increase to 0.0501 amp./cm². Our cathode is 5 cm² in area, so that it would be necessary to assume that 10^{-4} of its surface is on the average kept at 600°K by the ion bombardment in order that a change of 600 in b should give a change in emission of 16 microamperes. Probably the change in b is greater than this, for it is well known that the increase in current produced by field at these composite surfaces of low work-function is much greater than that calculated from the Schottky theory. It is necessary to account for some $20\mu a.$ of current by this extra secondary emission, and it appears that our theory is quantitatively possible, although by no means definitely proved by these calculations.

[10] Lukirsky and Prilezaev, Zeits. f. Physik **49**, 236 (1928).
[11] L. R. Koller, Phys. Rev. **33**, 1082 (1929).

Noise in Gas-Filled Cells

A few measurements were also made of the spontaneous disturbances occurring in the photo-cell current. A wire-wound resistance of 10^6 ohms was connected in series with the cell, and the voltage fluctuations across this resistance were amplified and measured. Unfortunately, the amplifier used was quite regenerative, so that its frequency response curve had a peak at 500 cycles, and fell to half value at 28 and 2700 cycles respectively on either side. The output readings of the amplifier were expressed as RMS voltages at 60 cycles across the input megohm, although these voltages do not have much absolute significance as very little is known about the frequency characteristics of the noise.

It was found that the noise input increased linearly with the photo-current, and was largest for cells having the largest gas amplification. Indeed it was found that the noise input was a linear function of the gas amplification factor of the cell, this factor being defined as the ratio of photo-current at voltage V to that at 25 volts, this latter current being practically the primary photo-emission of the cell. Fig. 8 shows the noise input for five different tubes, plotted as a function of gas amplification factor, each tube being run at

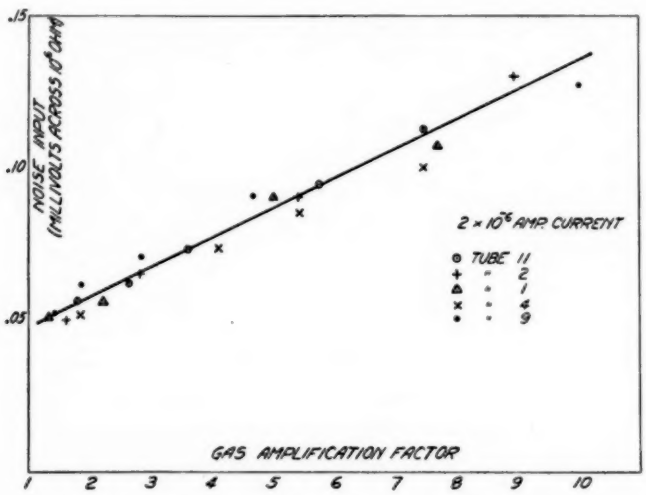

Fig. 8. Spontaneous "noise" in anode current of gas-filled photo-tube as function of gas amplification of photo-current.

several different voltages so as to get different values for this factor, and the light being adjusted in each case to give a current of 2×10^{-6} amp.

The obvious connection between the gas amplification and the noise suggests that the noise is similar to the "flicker effect" discussed by Johnson[12] and by Schottky,[13] and is due to the changes in work function of the cathode produced by the random impacts of the positive ions. This would attribute the noise to the same source as the lag effect discussed in the previous section.

[12] J. B. Johnson, Phys. Rev. **26,** 71 (1925).
[13] W. Schottky, Phys. Rev. **28,** 74 (1926).

Very little is known about the frequency characteristics of the photo-cell noise. Mr. Metcalf of this laboratory has made some measurements of the noise by using an amplifier giving good response from about 30 cycles up to one hundred thousand cycles. He found that the noise output of this amplifier was practically unchanged when a condenser was connected across the input, of sufficient size to short-circuit all frequencies above a few thousand cycles. Moreover, the absolute values of his input voltages were of the same order as ours, so there can be little doubt that the greater part of the noise spectrum lies below a few thousand cycles. This evidence thus supports the time-lag experiments in assigning a "life" of the order 10^{-3} sec. to the charge delivered to the cathode surface by an ion.

THE USE OF GLYCOL-PHTHALIC ANHYDRIDE RESIN AS A HIGH-VACUUM CEMENT[1]

By T. P. Sager and R. G. Kennedy, Jr.

Bureau of Standards, Washington, D. C.

(Received September 25, 1931)

Abstract

By using ethylene glycol-phthalic anhydride resin to seal the top of a camera box in a magnetic spectrograph it was found that a high vacuum could be obtained after pumping a short time. The preparation of the resin and its characteristics are described.

IN THE development of a magnetic spectrograph considerable difficulty was experienced in obtaining a cement which would permit the attainment of a high vacuum, essential for the satisfactory performance of the apparatus, after a reasonably short period of evacuation.

The apparatus consisted of an x-ray tube of a hot cathode type and a camera box connected by glass tubing to a vacuum train. Three mercury diffusion pumps backed by an oil-sealed mechanical pump were used. The vacuum readings were obtained with a Western Electric ionization manometer, an instrument which gives direct readings as low as 1×10^{-6} mm of mercury. After many refinements had been made in construction, it was possible to eliminate all greased joints. It was necessary, however, to seal the top of the camera box with a cement. The materials ordinarily recommended for this purpose either failed to maintain a sufficiently high vacuum or too much time was required before a high vacuum was obtained.

In the search for a suitable material it was found that the properties of some of the resins of the polyhydric alcohol-polybasic acid type appeared to meet our requirements. These resins have been in use commercially for some time. Only recently have systematic studies been made of the reactions involved.[2] It seemed desirable to employ the condensation product of ethylene glycol and phthalic anhydride. Since both of the reactants contain two functional groups, a product should be obtained which would have a high degree of esterification, with stability and low vapor pressure. The use of phthalic anhydride as the acid component would insure a resin having an amorphous structure and hence no sharp melting point.

In the preparation, no attempt was made to produce a resin of exceptional purity. A mixture of 124 g of ethylene glycol (boiling point 197°C) and 296 g of phthalic anhydride (stoichiometrical proportions) was gradually heated to 220°C and held at that temperature for eight hours, when a cooled

[1] Publication approved by the Director of the Bureau of Standards of the U. S. Department of Commerce.

[2] Carothers and Arvin, J. Am. Chem. Soc. **51**, 2568 (1929); Kienle and Hovey, J. Am. Chem. Soc. **51**, 509 (1929); **52**, 3636 (1930).

sample indicated by its clear, glass-like appearance that a condition approaching equilibrium had been reached. The flask was then removed from the bath and allowed to cool. The resinous product was found to be clear, amber colored, and readily fractured at room temperature. It had no sharp melting point but softened readily on warming and when heated on the steam bath was the consistency of balsam.

The resin had the following characteristics:

Free acid (as phthalic anhydride)	2.3 percent
Acid number	18
Ester number	559
Saponification number	577
Esterification	96.8 percent
Softening point (ring and ball method)	72°C

It was believed that volatile substances in cements were a factor in the length of time required to evacuate the apparatus. A comparison of the behavior of representative cementing materials was therefore made irrespective of their sealing ability. The x-ray tube and camera box were disconnected from the vacuum train and approximately the same volume of the materials to be tested was placed in a Pyrex tube and the tube sealed on to the end of the train. The vacua obtained when various materials were enclosed in the vacuum train are given in Table I. The pumping in each case was continued for 1.5 hours.

TABLE I.

Material	Pressure $\times 10^{-5}$ (mm of mercury)
Pyrex tube (blank)	0.45
Cement "A" (wax type)	6.8
Cement "B" (wax type)	4.9
Cement "C" (chicle type)	4.5
Rubber (cured)	3.2
Glycol-phthalic anhydride resin	1.1

A sample of glycol-phthalic anhydride resin was used repeatedly without any change in its properties. Since this material has been employed the operation of the spectrograph has proved successful, whereas formerly no distinct bands could be obtained on the photographic plate. The use of the resin prolonged the life of the tungsten filaments in the x-ray tube. When substances such as chicle were employed the filaments burned out after ten hours of operation. With the resin the filaments have not burned out after seventy hours of use.

The successful use of this material in a particular apparatus may suggest similar applications elsewhere. The resin has a conveniently low softening point and can be easily applied without overheating parts of the apparatus. It readily wets the surface of metals and glass. It is insoluble in ether, petroleum ether, alcohol, and water but dissolves in such substances as acetone and ethyl acetate. At room temperature it has a rigidity and mechanical strength comparable with hard cements customarily used.

THE TIME LAG OF THE ELECTRIC SPARK

By John A. Tiedeman

Rouss Physical Laboratory, University of Virginia

(Received September 21, 1931)

Abstract

The variation in the time lag of the electric spark has been investigated as a function of the applied field and the number of electrons liberated at the cathode by ultraviolet light, during the application of the field. The time intervals were measured by a Lichtenberg figure method with a precision of 5×10^{-10} sec. A biasing positive potential was applied to the zinc cathode in such a way that not only were the residual ions removed from between the electrodes before the application of the field but a known number of electrons could be liberated from the cathode by ultraviolet light while the field was applied. For the case of air, hydrogen, and nitrogen curves are given showing how the time lag decreases with an increase in the number of electrons liberated during the application of the field. It is shown that with comparatively high applied fields the time lag reduces to approximately the time required for an electron to be liberated in the gap.

THE time lag of the electric spark may be defined as the length of time which elapses between the instant when the breakdown potential is reached, and the instant when the breakdown itself begins. Although this is the usual definition it is hard to realize practically, since recent work on the fate of fall of potential in a spark gap demonstrates that in the initial stages of the discharge the rate of fall is very gradual. While it takes roughly 10^{-8} seconds for the potential to fall the first 10 percent of the full value, it takes only about 10^{-9} seconds for the potential to fall the next 10 percent. It is one of the advantages of the method of investigation used here that the time is measured from the instant the applied potential wave exceeds 2700 volts until breakdown begins.

In 1887 Hertz[1] discovered that the discharge of a spark gap "takes place more readily" when it is illuminated with ultraviolet light. Herweg,[2] on the bases of his experiments, thought that the explanation lay in a lowered breakdown strength of the gap caused by the action of the light. More careful experiments by Warburg[3] demonstrate that this is not the case, and that the breakdown field strength was practically constant even if enormous variations in the intensity of the light were made.

Even up to the present time the role played by the ultraviolet radiation in the time lag of the spark is not thoroughly determined. Some experimental work has been interpreted as showing that, although there is a difference in the time lag of gaps which are illuminated and those which are not, variations

[1] H. Hertz, Berl. Ber. 487 (1887).
[2] Herweg, Ann. d. Physik **24,** 326 (1907).
[3] E. Warburg, Verh. deut. Phys. Ges. **2,** 212 (1900).

in intensity of the light do not produce changes in the time lag. The work described here was undertaken as a means of reconciling contradictions which had arisen from the work of previous investigators.

Time lags have been measured by Zuber,[4] Pederson,[5] Regener,[6] Beams,[7] Rogowski,[8] and in the last few months by Viehman.[9] Pederson worked over a wide range of pressures and voltages and, although he found that the time lag depended on the electric field applied in the gap, he did not discover a relation between the intensity of the irradiation and the time lag. The work of Zuber, however, shows that there is a definite dependence of the time lag on the intensity of irradiation, as well as on the amount of voltage applied above the normal sparking voltage. But his work was confined to gases at low pres-

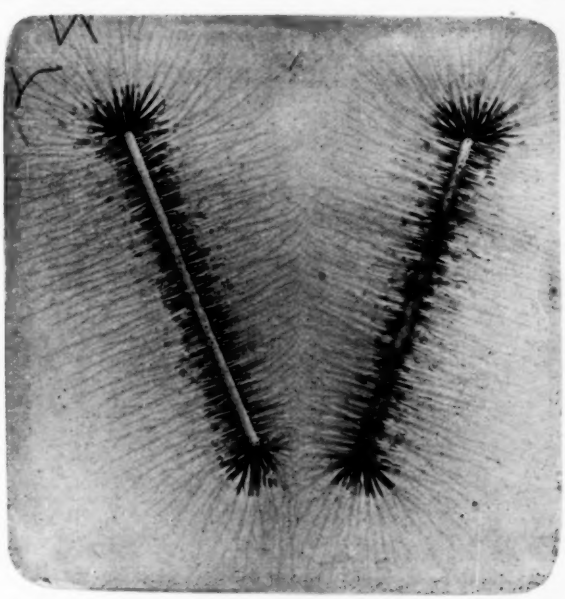

Fig. 1. Specimen of Lichtenberg figure applied to the measurement of time intervals.

sures and with consequent low voltages applied to his gaps. Viehman, whose paper appeared since the work reported here was completed, shows also a difference in the time lags with and without irradiation, but does not study the effect of changes in the intensity of irradiation used. The work of all the above experimenters, though in agreement as to the order of magnitude of the time lag, present wide discrepancies as to the exact effect of irradiation on the time lag.

To study the factors affecting the time lag a method similar to that used by Pederson was adopted, though differing from it in several important par-

[4] K. Zuber, Ann. d. Physik **76,** 231 (1925).
[5] P. O. Pederson, Ann. d. Physik **71,** 317 (1923).
[6] Hiller and Regener, Zeits. f. Physik **23,** 129 (1924).
[7] J. W. Beams, Jour. Frank. Inst. **206,** 809 (1928).
[8] W. Rogowski, Archiv f. Elektrotech. **16,** 496 (1926).
[9] H. Viehman, Archiv f. Elektrotech. **25,** 253 (1931).

ticulars. The method is based on the use of the Lichtenberg figure. The simple Lichtenberg figure can be produced by placing an electrode on the emulsion of a photographic plate. At the back of this is placed a metal grounded plate. If the potential difference between the electrode and the grounded plate is suddenly raised to a value in excess of 2700 volts, there will be found on the photographic plate after it is developed a characteristic figure known as the Lichtenberg figure. These figures[10] have been used commercially in the measurement of surge voltages, but Pederson was the first to use them for the measurement of time intervals. He found that the figure streamers grew out from the electrode with a definite velocity, and that if two electrodes were placed close together and were excited from the same potential source, the figure from one electrode would grow only until it met the one which started from the other electrode. A definite and straight dividing line resulted, and

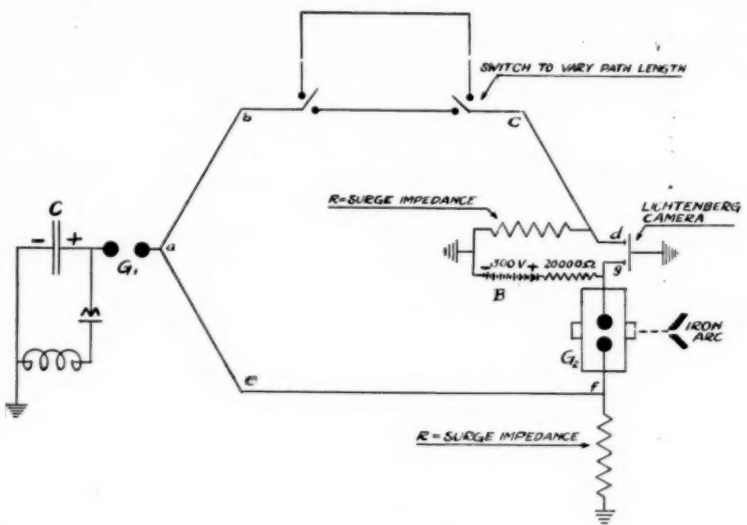

Fig. 2. Circuit diagram.

he found that the position of this dividing line was changed if the circuit was arranged so that the potential wave reached one electrode before it reached the other. (See Fig. 1).

The arrangement used for calibration is shown in Fig. 2. A condenser C is charged to a high positive potential sufficient to break down the gap G_1. When this gap breaks down a potential wave travels along the wire paths *abcd* and *aefg*. *d* and *g* are the electrodes which rest upon the photographic plate. If these paths are the same in length, and if the spark gap G_2 is shorted with a conductor, one potential wave will arrive at the electrode *d* at the instant the other arrives at the electrode *g*. When the photographic plate is now removed from the camera and developed it will be found to bear a figure similar to Fig. 1, with the dividing line lying midway between the traces of the elec-

[10] P. O. Pederson, Vid. Selsk. Math. Fys. Medd. Kopenhagen, **1,** 11 (1927); E. S. Lee and C. M. Foust, Gen. Elec. Rev. **30,** 135 (1927).

trodes. By inserting a longer wire path between *b* and *c* and taking another figure it will then be found that the dividing line will lie closer to the electrode *d* than to the electrode *g*. When the path length differed by three meters, an interval of time equal to 10^{-8} sec., (assuming that the velocity of the electric wave along the wire is equal to the velocity of light), it was found in the apparatus used in this experiment that the dividing line of the figure was displaced 4 mm. Since the electrodes were 12 mm apart at their nearest tips, a displacement from the tip of one to the tip of the other represented a time interval of 3×10^{-8} sec. The dividing line could be located to within 0.2 mm, so that the device was precise in this range to 5×10^{-10} sec. The calibration is not linear when the dividing line does not lie in the portion between the electrodes, nor can measurements be made so accurately. In calibrating, as well as in making the time lag measurements, it was found necessary to change the wire path by adding and removing definite lengths of wire.

The wire paths *abcd* and *aefg* were terminated by the resistances *R* which were adjusted by experiment to equal the surge impedance of the lines to eliminate reflected waves from the ends.

Since the velocity with which the figure streamers are formed depends on the potential impressed on the electrodes it is necessary to make a new calibration for each potential which is used. To avoid this complication the gap G_1 was kept at the same setting, and was illuminated with the light from an iron arc to minimize its time lag. In a few experiments the setting of this gap was changed so that the voltage applied was 26.5 instead of 16.7 kv, the latter being the voltage used in most of the experiments. It was found that the same calibration could be used even in this case if the camera electrodes, instead of being connected directly to the end of the line, were connected at such points of the terminal resistances *R* that the potential of *d* and *g* to ground was reduced to 16.7 kv.

The use of the Lichtenberg figure as a measuring device requires that the potential applied to the gap be a surge potential. Varying amounts of overvoltage could be applied by changing the setting of the gap G_2. Field strengths as high as seven times the normal breakdown field strengths were used in this experiment. It is only because great care was taken in providing voltages to sweep out the ions and shielding for the gap that such high field strengths could be obtained.[11] These high field strengths could be applied to the gap without breakdown only in the absence of ultraviolet light. The fact that the gap does not break down at these high field strengths when it is not illuminated, indicates that its time lag is well in excess of 10^{-6} seconds, because the potential wave used maintains the potential of the gap in excess of the normal breakdown voltage for at least that length of time at the high field strengths.

Fig. 3 shows the design of the spark gap used in this experiment. A 16 mm steel sphere was used as the anode, and a 16 mm zinc sphere was used as the cathode. The shaft of the steel sphere was set in a disk of bakelite, which had been machined to fit the end of the brass cylinder. The shaft of the zinc sphere was set in a second bakelite disk, further insulated with a ring of sul-

[11] Street and Beams, Phys. Rev. **38**, 425 (1931).

fur, so that measurements of the photoelectric emission of the zinc under the action of various intensities of ultraviolet light could be made. Two brass tubes were soldered in opposite sides of the cylinder; one of these was covered with a quartz plate, so that the ultraviolet light could be admitted, and the other was closed with a glass window. This window served to locate the light source with respect to the spheres by sighting through the gap.

Preliminary experiments demonstrated that the time lags would not vary with light intensity unless elaborate precautions were taken to limit the number of electrons in the gap. Since there are numerous electrons and ions in the gap due to the irradiation, the number present at any time will not bear a definite relation to the light intensity unless care is taken to sweep them from the gap as soon as they are formed. In fact, it is probably because previous investigators had not thoroughly eliminated the residual ionization that the effect of irradiation on the time lags was not cleared up.

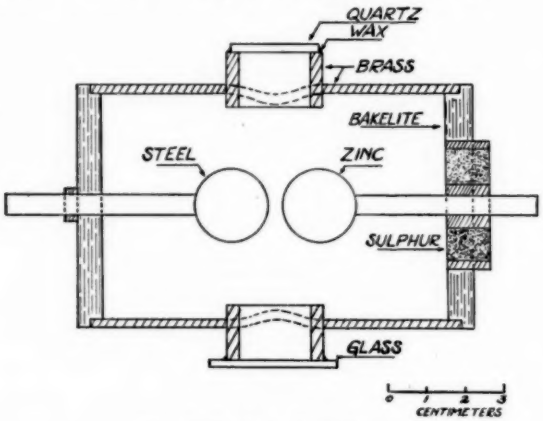

Fig. 3. Design of spark gap.

The electrode of the gap G_2 (See Fig. 2) nearer the camera was kept at a positive potential of 300 volts. No electrons would be liberated from it until the surge potential in the gap arose to a value in excess of this. This electrode was made of zinc, which has a high photoelectric emission in the ultra-violet range used. No electrons were liberated from the other electrode for it was made of steel, which has a threshold value in the ultraviolet far beyond this range. This bias voltage was produced by connecting the battery B as indicated through a resistance of about 20,000 ohms.

It was a simple matter to check the ionization conditions in the gap with this arrangement. When the gap G_1 broke down, a discharge would occur in the gap G_2 only when it was irradiated. In order to determine whether conditions in this gap were satisfactory for taking data, the gap G_1 was allowed to break down about twenty times a minute and, with irradiation, the gap G_2 would also break down each time. If conditions in the gap were good for taking data, the gap G_2 would no longer break down if a screen were interposed between it and the light source. If this test showed that conditions in the gap were satisfactory the Lichtenberg camera was connected to the circuit, and photographic records were made of single sparks.

At first lantern slide plates were used in the camera, but when it was found necessary to take a large amount of data under each condition, it was decided to use a long roll film. A camera was designed in which the film traveled over a glass plate which was backed by a brass plate connected to ground. The electrodes were mounted on a plate of insulating material and were pressed against the film by springs. When it was desired to change the position of the film for a new exposure, a lever on the top of the box was used to raise the electrodes clear of the film. The film could then be moved so that a new surface came under the electrodes. By releasing the lever, the electrodes would again press the film against the glass plate, and the camera would be ready for another exposure. A 42″×5″ film was used, arranged so that 36 to 45 exposures could be made on one film.

An iron arc run on 220 volts d.c. at five amperes was used as the ultraviolet light source. The intensity of irradiation could be varied by changing the distance from the gap. Measurements of the emission current from the

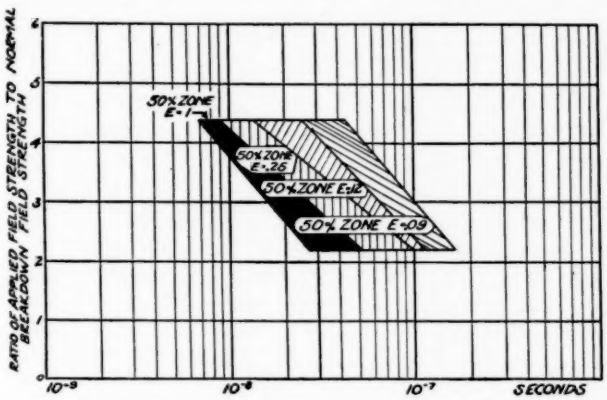

Fig. 4. Time lag as a function of overvoltage for various light intensities in air. Maximum applied voltage 26.5 kv.

zinc for various light intensities were made by means of a standard condenser and an electroscope. From these data the number of electrons emitted per second was calculated.

It was found that when a very intense light source was used all the measurements of time lag were short, and that they differed among themselves by little more than the errors of measurement. With less intense light, the shortest time lags would be as short as those obtained with the intense light, but there would be a great number which were longer than any which had been obtained before. On the basis of the Townsend theory of the spark discharge it is necessary to have a few electrons in the gap before the breakdown will occur. With intense light there will always be electrons present to initiate the discharge, but with a weak intensity enough electrons to precipitate the discharge may not be liberated for some period of time.

Fig. 4 shows the results of the experiments in air with an applied voltage of 26.5 kv. The ordinate is the ratio of the field strength applied to the gap to the field strength at which the gap will just break down under a steady field.

The data were taken at two field strengths, in which the ratio of G_1 to G_2 was 4.4 and 2.2 respectively, and each of these with four different light intensities. To simplify the diagram we are considering only half the measurements, and we choose the shortest time lags measured under each condition, discarding the longer ones for the present. The inclusion of all the measurements at this point would merely confuse the diagram without appreciably changing the conclusions. With the most intense light used, (light which would liberate 10^8 electrons per second is shown on all the diagrams by $E=1$), 50 percent of the time lags fell in the black region, and the 50 percent which we are disregard-

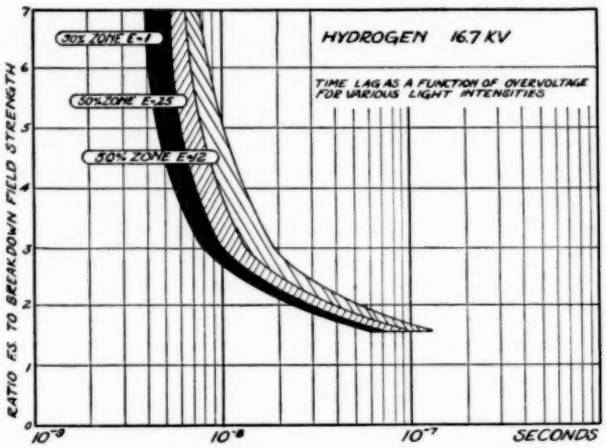
HYDROGEN 16.7 KV
TIME LAG AS A FUNCTION OF OVERVOLTAGE FOR VARIOUS LIGHT INTENSITIES
50% ZONE E=1
50% ZONE E=.25
50% ZONE E=.12
RATIO FS TO BREAKDOWN FIELD STRENGTH
SECONDS

Fig. 5. Time lag as a function of overvoltage for various light intensities in hydrogen. Maximum applied voltage 16.7 kv.

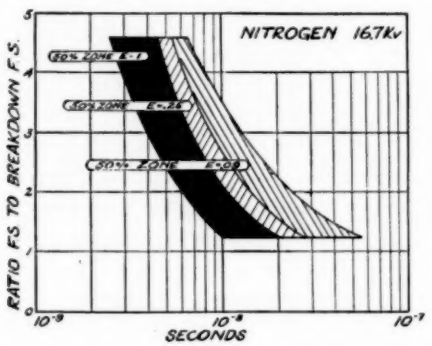

Fig. 6. Time lag as a function of overvoltage for various light intensities in nitrogen. Maximum applied voltage 16.7 kv.

ing fell to the right of the black region. With a less intense light (which would liberate one fourth as many electrons, $E=0.25$), 50 percent of the time lags fell in the region comprised of the black zone and the zone which is cross-hatched vertically. When an intensity $E=0.12$ was used, 50 percent of the time lags fell in a region comprised of the first three zones, and with $E=0.09$ 50 percent of the time lags fell in the region comprised of all four sections. The anomalous slope of the border of the vertically cross-hatched section may

possibly be due to an error in measuring the light intensity, as this slope is very sensitive to small errors of this kind.

Figs. 5 and 6 are diagrams similar to Fig. 4, but the data for these were taken in nitrogen and hydrogen respectively and with an applied voltage of 16.7 kv. The applied field strengths used in these gases were lower than those used in Fig. 4, and it is to be noticed that as the ratio of the field strengths applied approaches unity, that is, when the applied field strength exceeds the normal breakdown field strength by only a small amount, the time lags become very long. This same effect was observed in air, though sufficient data were not obtained to allow it to be shown on Fig. 4.

von Laue[12] has considered the statistical distribution in time which might be expected from a number of time lag measurements. He finds that

$$\log n_t^{\infty} = -\rho \int_0^t p(t)dt$$

in which n_t^{∞} is the number of time lag measurements each of which exceeds t; $p(t)$ is a function representing the probability that with an electron in the gap a discharge will take place in a time range of t to $t+dt$. We may express this law in terms of the percent of the total number of observations in excess of the value t, rather than in terms of the total number. Then

$$\log \frac{100}{N} n_t^{\infty} = -\rho \int_0^t p(t)dt + c.$$

Assuming that $p(t)$ does not depend on the time, the integration can be performed directly and we have

$$\log \frac{100}{N} n_t^{\infty} = -\rho p(t)t + c.$$

Zuber found in his work that the quantity ρ corresponded to the number of electrons emitted per second, and that $p(t)$ increased with increasing voltage applied to the gap in excess of the normal breakdown voltage. On a logarithmic graph the product $\rho p(t)$ represents the slope of the curve.

In order to compare the present results with the results of Zuber, the data were plotted in a similar manner. This is a matter of some interest as the data in the two experiments were taken under widely different conditions; Zuber's work was in gases at low pressures with low applied voltages, and time lags of the order of magnitude of a second were measured. On the other hand, the present work was in gases at atmospheric pressure, with high voltages applied, and high overvoltages, and time lags beyond the order of 10^{-7} seconds were not measured.

To make a comparable plot we must list all the observations made at any one field strength and light intensity in the order of ascending magnitude. We list first the shortest time lag measured, then the one which is next longer, and so on for the whole series of measurements. Since all the observations were as long as, or longer than our first value, we will plot this value with an ordinate

[12] von Laue, Ann. d. Physik **76**, 261 (1926).

of 95 percent, and would continue in this way until we had plotted all our observations, assuming that twenty observations had been made.

Figs. 7 and 8 are plotted in this way. Four light intensities are plotted on each curve. All the data on Fig. 7 were taken at a field strength of 140 kv/cm,

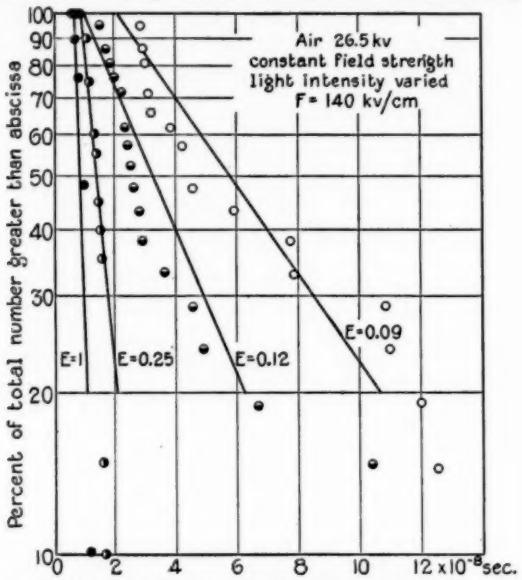

Fig. 7. Variation of time lag with light intensity in air. Maximum applied voltage 26.5 kv. Maximum field strength applied 140 kv/cm.

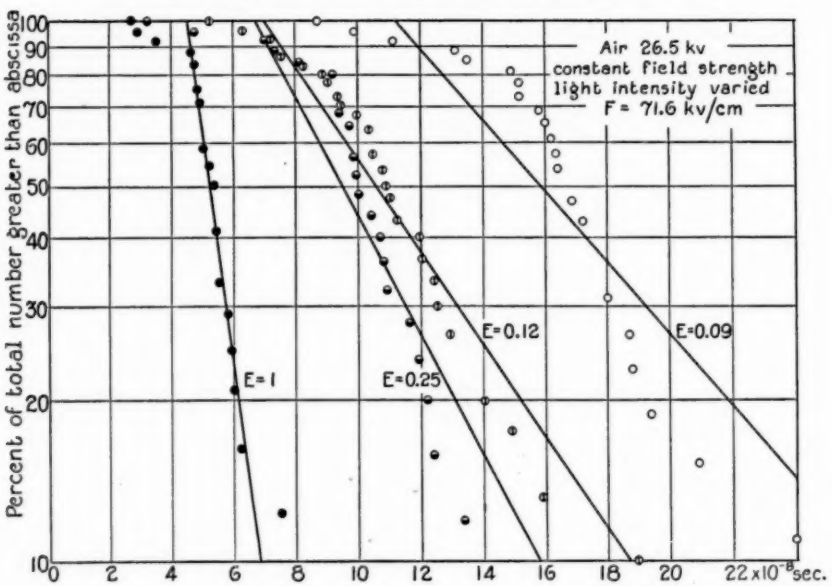

Fig. 8. Variation of time lag with light intensity in air. Maximum applied voltage 26.5 kv. Maximum field strength applied 71.6 kv/cm.

and the data shown on Fig. 8 were taken at a field strength of 71.6 kv/cm. It will be observed that the slopes of these curves increase with increasing light

intensity, and with increased field strength. These changes in the slope are similar to those found by Zuber in his experiments. In a general way the slopes follow the relation

$$s = kE(F - f)$$

in which s is the slope, k is a constant, E is 10^{-8} times the number of electrons liberated on the average per second, F is the field strength applied, and f is the normal breakdown field strength. It was found that the data could be represented equally well by the relation

$$s = k'E\alpha d$$

where α is the number of electrons which will be formed by the travel of an electron through one centimeter under the action of the electric field applied to the gap, d is the spacing of the gap in centimeters, E has the significance above, and k' is another constant.

Table I lists the slopes of all the curves taken as well as the abscissae of their intersections with the 100 percent level, which in this table are called the minimum time lags.

TABLE I. *General summary of results.*

AIR

Field strength varied—Maximum potential 16.7 kv.

Field strength kv/cm F	Minimum time lag $\times 10^{-8}$ sec. T	Slope s	
155	1.0	0.50	
77	1.5	0.38	
62	3.5	0.16	Light intensity
51	5.0	0.14	$E=2$ for each case.
42	8.4	0.07	

Variation of light intensity—Maximum potential 16.7 kv.

Light intensity Electrons/sec. $\times 10^8$ E^*	Minimum time lag $\times 10^{-8}$ sec. T	Slope s	
2.0	1.5	0.38	Field strength
0.4	2.3	0.28	$F=77$ for each case.
0.2	2.6	0.13	

Maximum potential 26.5 kv.

Field strength kv/cm F	Light intensity Electrons/sec. $\times 10^8$ E	Minimum time lag $\times 10^{-8}$ sec. T	Slope s
140	1.0	0.7	3.3
140	0.25	0.9	1.1
140	0.12	1.0	0.26
140	0.09	2.2	0.16
72	1.0	4.5	0.83
72	0.25	6.8	0.21
72	0.12	7.0	0.16
72	0.09	11.2	0.13

TABLE I. (*Cont.*)

HYDROGEN

Maximum potential 16.7 kv.

Field strength kv/cm F	Light intensity Electrons/sec. $\times 10^8$ E	Minimum time lag $\times 10^{-8}$ sec. T	Slope s
110	1.0	0.45	5.0
110	0.25	0.65	3.3
110	0.12	0.70	2.2
55	1.0	0.9	4.0
55	0.25	1.1	1.8
55	0.12	1.4	1.4
55	0.9	1.5	1.2
27.5	1.0	7.0	3.3
27.5	0.25	7.2	1.3
27.5	0.09	8.0	0.44
27.5	0.03	9.2	0.20

NITROGEN

Maximum potential 16.7 kv.

Field strength kv/cm F	Light intensity Electrons/sec. $\times 10^8$ E	Minimum time lag $\times 10^{-8}$ sec. T	Slope s
160	1.0	0.46	12.0
160	0.25	0.47	11.5
160	0.09	0.71	4.9
67	1.0	—	4.0
67	0.25	0.68	1.5
67	0.09	0.72	1.0
42	1.0	1.38	0.88
42	0.25	1.62	0.41
42	0.09	1.76	0.14

* E represents the number of electrons liberated per second.

Although the relations given above hold for the average slopes as drawn, the straight lines do not fit the experimental data very well. Two explanations may be advanced. In the first place, the field strength in this experiment is not constant, but changes with the time. It is nearly constant from about 6×10^{-8} sec. to about 20×10^{-8} sec. after which it begins to decrease. In Zuber's work the applied field strength was but a few volts in excess of the normal breakdown field strength, and the assumption that the function $p(t)$ was independent of the time was apparently justified. Since we find that the slopes of the curves change with the overvoltage applied, and since the voltage changes with the time, we could hardly expect that the function $p(t)$ is independent of the time in this experiment. But the second explanation seems to be more important. In this experiment the time lags measured are of the same order of magnitude as the average time which elapses between the liberation of electrons. Most of the interval included in the time lags measured here consists of the time which must elape before there is an electron present in the gap to initiate the discharge. It is to be noted that only an average time between the emission of electrons can be calculated from the measurements of

the gap current. With this in mind we cannot expect that the probability function $p(t)$ will be independent of the time, and we would expect a considerable departure from the results of Zuber. von Laue has shown that, in using this method of plotting, the average value of the time lag is given by the 37 percent ordinate. Our curves are steep in this portion, and the value of time lag for the experiments in air is just one half of the average time between electrons. We can then conclude that with high overvoltages each electron emitted is sufficient to initiate a discharge. Therefore, the time necessary to establish the discharge is shorter than the average time between the ejections of electrons from the cathode.

This does not necessarily hold for the measurements in nitrogen and hydrogen because in these gases measurements of the emission were not made directly. Since it was found convenient to evacuate the gap in order to fill it with a different gas, the sulfur insulation was replaced, and consequently it became impossible to make a measurement of the average number of electrons liberated per second. The values for the average numbers of electrons used were figured from the measurements made with air in the gap and may not be applicable. It is clear that the phenomenon has the same general trend in nitrogen and in hydrogen as it has in air, even if it is not possible to interpret the results in terms of the number of electrons liberated.

von Hippel and Franck[13] have advanced a theory for the time lag. However, since on their theory, any field strength in excess of 45 kv/cm will produce breakdown in the time necessary for one electron to cross the gap, it is not easy to check their theory quantitatively. The evidence, as far as it goes, is in agreement with their theory.

There is a possibility that there may be more electrons in the gap than we have calculated. However, the maximum time that an electron liberated with a velocity equivalent to two volts (which is about the right value for zinc illuminated as in this experiment) can remain in a gap with a field strength such as that used for a bias potential is about 2×10^{-10} sec., a time small in comparison with the average time between ejections of electrons in the present case. A further possibility exists in that some electrons may be attached to molecules, and that such electrons might conceivably initiate the discharge when the field strength is raised. Basing a calculation on the attachment and mobility data given by Loeb[14] we find that this is probably not the case. The probable distance at which attachment would occur has been calculated, and although there will be about a thousand attachments a second, ions so formed will persist in the gap less than 10^{-7} seconds, and we conclude that there will be less than one ion on the average in the gap at any time.

The author takes pleasure in acknowledging his indebtedness to Dr. Jesse W. Beams, under whose direction the work reported here was carried out, as well as his gratitude to Dr. L. G. Hoxton whose advice and cooperation were of great value.

[13] von Hippel and Franck, Zeits. f. Physik **57**, 696 (1929).

[14] Loeb, Kinetic Theory of Gases, pp. 504, and 513 (1927).

A NEW METHOD OF DIELECTRIC CONSTANT MEASUREMENT AT RADIO FREQUENCIES

By H. L. Andrews

Department of Physics, Brown University

(Received October 8, 1931)

Abstract

A new method of making dielectric constant measurements on gases at radio frequencies is described. This method eliminates the difficult condenser calibration required by earlier heterodyne methods. In addition, the effect of certain errors in previous methods can be estimated. The dielectric constant is obtained in terms of a single frequency standard, whose absolute frequency can be determined by auxiliary apparatus described. The method has been used to measure the dielectric constant of nitrogen at room temperature over a pressure range from zero to seven atmospheres. All measurements were made at a frequency of 884 kilocycles. The final value of $\epsilon-1$ at N.P.T. $=0.000589$ is probably correct in absolute value to better than 0.5 percent.

Introduction

In SPITE of the development of the modern vacuum tube as a powerful research tool, there is a lack of agreement in dielectric constant data as obtained by different observers. One set of observations may be self consistent, but may differ from the results obtained with another apparatus by several times the estimated errors of measurement. This is particularly true in the case of gases, whose dielectric effect is in general very small. From a theoretical standpoint, however, the dielectric constants of gases are particularly important. The present investigation was undertaken in the hope that some of the discrepancies might be eliminated, and a method of measurement developed which could be depended upon to give accurate absolute values of dielectric constants at radio frequencies. The method was developed for work with gases because of their theoretical significance, but with a few modifications it should prove useful in the study of liquid dielectrics. In order to show the advantages of the present method the essential features of the earlier vacuum tube methods will be briefly discussed.

Method of Measurement

One of the most successful methods of dielectric constant measurement is that first used by C. T. Zahn.[1] Two vacuum tube oscillators were used, each operating at a frequency of about one million cycles. One of these was kept at a constant frequency while the second contained the condenser to which gas was admitted. The tuned circuit of the second oscillator is shown in Fig. 1. In operation condenser C was evacuated, and the oscillators adjusted until

[1] C. T. Zahn, Phys. Rev. **24**, 400 (1924).

the heterodyne beat note gave zero beats with an auxiliary tuning fork. When gas was admitted to C a readjustment of K returned the beat note to zero beats with the tuning fork. The condenser arrangement magnified the capacity increase so that the change in K became many times the change in C.

In order to obtain an absolute value of the dielectric constant it is necessary to know the initial capacity of the condenser C as well as the capacity K' and all lead capacities. This involves a careful calibration in terms of condenser K, a variable condenser whose calibration is known. In calibrating C it is impossible to avoid measuring also the capacity through the insulators

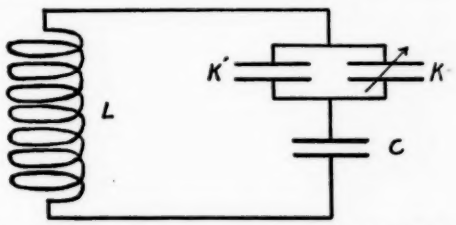

Fig. 1. The condenser arrangement used by Zahn.

of this condenser. As this capacity is unaltered upon the admission of gas it is necessary to correct for this error. This, together with the rather difficult determination of lead capacities, may cause an error in the final value of the dielectric constant. The effect of inductance of the leads to condenser C cannot be determined and is assumed to be negligible.

It should be noted that the sources of error tend to give an inaccurate value for capacity C. An error of this kind could not be detected by measurements with a single apparatus. All values would be self consistent, but might contain an error in absolute value. The new method is such that errors of this sort can be detected, while the condenser calibration, which is at best a laborious process, is entirely eliminated.

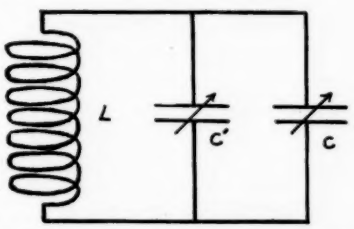

Fig. 2. The tuned circuit used in the present method.

In the present arrangement the beat note formed between a vacuum tube oscillator and an harmonic of a crystal oscillator is amplified and impressed on one pair of plates of a cathode-ray oscillograph tube. The output of a continuously variable audio-frequency oscillator is impressed on the second pair of plates.

Fig. 2 shows the arrangement of the tuned circuit of the tube oscillator. The gas condenser C consists of a variable radio condenser having a maximum capacity of about 700 micromicrofarads. The construction of this condenser

will be discussed in detail later. Condenser C' is a General Radio precision condenser with a maximum capacity of 1500 micromicrofarads.

It can be shown[2] that the oscillation frequency of a tuned plate oscillator, such as was used in this work, is given by

$$f = \frac{1}{2\pi}\left(\frac{1}{LC}\left(1 + \frac{R_L}{R_P}\right) - A^2\right)^{1/2} \tag{1}$$

where L is the inductance in the oscillating circuit, C the total capacity in the oscillating circuit, R_L the effective resistance of the oscillating circuit, R_P the plate resistance of the tube and A a factor depending on the tube constants and the mutual inductance between grid and plate circuits. In practice the oscillator was so adjusted that the term A became small. Care was also taken to make R_P very large and R_L as small as possible. Then the quotient R_L/R_P will be small under all operating conditions, and can be considered constant over a considerable frequency range. Then (1) becomes

$$f \alpha \frac{1}{C^{1/2}}$$

or

$$C = \frac{a}{f^2} \tag{2}$$

where a is a constant depending on the construction of the apparatus.

In making a dielectric constant determination gas condenser C is evacuated and set to approximately its maximum capacity, and variable condenser C' adjusted until the tube oscillator produces an audio-frequency beat note with any desired harmonic of the crystal. Care is taken to form the beat note so that the tube oscillator frequency is lower than the frequency of the crystal harmonic. Let that portion of the total capacity which is altered by the admission of gas be denoted by C_{11}. All other capacity in the tuned circuit will be denoted by C_{01}. Thus C_{01} includes the capacity of the precision condenser C', all lead capacities, and that portion of C which is unaffected by the admission of gas. Then by (2)

$$C_{11} + C_{01} = \frac{a}{f_{11}^2}. \tag{3}$$

Since the tube oscillator is working at a frequency slightly less than the frequency of the crystal harmonic

$$f_{11} = n_1 f_c - f_{A_1} \tag{4}$$

where n_1 is the number of the crystal harmonic, f_c the fundamental frequency of the crystal and f_{A_1} the audio frequency required to form a 1:1 Lissajous figure with the beat note.

Gas is now admitted to the gas condenser. The resulting capacity increase decreases the tube oscillator frequency, which increases the beat note frequency. The new conditions are given by

[2] J. H. Morecroft, Principles of Radio Communication, 569.

$$C_{12} + C_{01} = \frac{a}{f_{12}^2}. \tag{5}$$

Corresponding to (4) we now have

$$f_{12} = n_1 f_c - f_{A_2}. \tag{6}$$

Subtracting (3) from (5)

$$C_{12} - C_{11} = a\left(\frac{1}{f_{12}^2} - \frac{1}{f_{11}^2}\right)$$

which may be written

$$C_{12} - C_{11} = a\left(\frac{f_{11} + f_{12}}{f_{11}^2 f_{12}^2}\right)(f_{11} - f_{12}). \tag{7}$$

Now the difference between f_{11} and f_{12} is small compared to either of them, so f_{12} may be replaced by f_{11} in the first factor. By (4) and (6) the second factor reduces to the difference of the audio frequencies. With these changes (7) becomes

$$C_{12} - C_{11} = \frac{2a}{f_{11}^3}(f_{A_2} - f_{A_1}). \tag{8}$$

Now by the definition of dielectric constant

$$\epsilon - 1 = \frac{C_{12} - C_{11}}{C_{11}} \tag{9}$$

Putting this in (8)

$$(\epsilon - 1)C_{11} = \frac{2a}{f_{11}^3}(f_{A_2} - f_{A_1}). \tag{10}$$

The capacity of condenser C is now greatly reduced with gas still between the plates. This capacity is adjusted until the tube oscillator gives a low audio-frequency beat note with some higher harmonic of the crystal. Conditions are now given by

$$C_{21} + C_{01} = \frac{a}{(n_2 f_c \pm f_{A_2})^2}. \tag{11}$$

This is written on the assumption that C_{01} does not change when the condenser setting is changed. Very careful bridge measurements justify the assumption, at least to an accuracy as great as is required.

The oscillator frequency is now brought back to form a low audio-frequency beat note with the original crystal harmonic n_1. This is done by increasing C', care being taken to form the beat note with the oscillator frequency higher than the frequency of the crystal harmonic. Then

$$C_{21} + C_{02} = \frac{a}{f_{21}^2} \tag{12}$$

where

$$f_{21} = n_1 f_c + f_{A_4} \tag{13}$$

The condenser is now re-evacuated. The final conditions are given by

$$C_{22} + C_{02} = \frac{a}{f_{22}^2} \tag{14}$$

$$f_{22} = n_1 f_c + f_{A_5}. \tag{15}$$

Substracting (14) from (12) and reducing as before

$$(\epsilon - 1)C_{22} = \frac{2a}{f_{22}^3}(f_{A_5} - f_{A_4}) \tag{16}$$

Eq. (16) is subtracted from (10)

$$(\epsilon - 1)\,(C_{11} - C_{22}) = 2a\left[\frac{f_{A_2} - f_{A_1}}{f_{11}^3} - \frac{f_{A_5} - f_{A_4}}{f_{22}^3}\right] \tag{17}$$

Eq. (17) contains two unknown capacities as well as the circuit constant a, but all of these may be eliminated by the use of the information obtained when the setting of C was changed.

For the first setting of C

$$C_{11} + C_{01} = \frac{a}{(n_1 f_c - f_{A_1})^2} \tag{18}$$

and for the second setting

$$C_{21} + C_{01} = \frac{a}{(n_2 f_c \pm f_{A_3})^2}. \tag{19}$$

Subtracting (19) from (18)

$$C_{11} - C_{21} = a\left[\frac{1}{(n_1 f_c - f_{A_1})^2} - \frac{1}{(n_2 f_c \pm f_{A_3})^2}\right]. \tag{20}$$

Now the difference between C_{21} and C_{22} is just the dielectric effect of the gas and this difference is small compared to C_{21}. Hence C_{21} may be replaced by C_{22} and we have

$$C_{11} - C_{22} = a\left[\frac{1}{(n_1 f_c - f_{A_1})^2} - \frac{1}{(n_2 f_c \pm f_{A_3})^2}\right]. \tag{21}$$

With this last relation (17) reduces to

$$\epsilon - 1 = 2\left[\frac{(n_1 f_c - f_{A_2})^2 (n_2 f_c \pm f_{A_3})^2}{(n_2 f_c \pm f_{A_3})^2 - (n_1 f_c - f_{A_2})^2}\right]\left[\frac{f_{A_2} - f_{A_1}}{(n_1 f_c - f_{A_1})^3} - \frac{f_{A_5} - f_{A_4}}{(n_1 f_c - f_{A_5})^3}\right] \tag{22}$$

Eq. (22) shows that it is possible to obtain $(\epsilon - 1)$ entirely in terms of frequencies. It is not necessary to know any of the capacities to a high degree

of accuracy and so the troublesome condenser calibration is completely eliminated. In addition this method furnishes a means of estimating the disturbing effects of some of the factors previously mentioned.

It should be noted that all of the measurements of the dielectric effect are made at the frequency of harmonic n_1. Harmonic n_2 is used merely as a reference point so that the capacity of C may be changed by a known amount. Moreover, both n_1 and n_2 are at the disposal of the operator, and may be varied within fairly wide limits. In the actual experimental set up n_1 could be varied from the 8th to the 15th harmonic of a 98.2 kc crystal. Corresponding to these values of n_1, n_2 could be chosen from 9 to 24. Since it is possible to work the procedure in reverse order, making the actual measurements on n_2 and using n_1 only for reference, a single set up allows measurements to be made in steps of 98.2 kc from 786 kc to 2357 kc.

The ability to choose harmonics n_1 and n_2 within reasonable limits is a very important feature. A series of measurements can be made, by using the same value of n_1, but with varying values of n_2. Since the shift from n_1 to n_2 is essentially a determination of the initial capacity of the gas condenser, a series of measurements of this sort should give some idea of the magnitude of the factors disturbing this quantity. These factors would not be expected to be proportional to the amount of frequency shift from n_1 to n_2. If the dielectric constant turns out to be independent of the shift it seems reasonable to believe that this will be a true dielectric effect only.

A still further check can be obtained by another series of measurements. Both n_1 and n_2 may be kept constant, each determination being made with a different initial capacity in the gas condenser. The disturbing effect of stray capacities, lead inductance and condenser leakage should be more pronounced for small values of the gas condenser capacity, since the magnitudes of these quantities remain approximately constant for all condenser settings. If the dielectric effect turns out to be a function of the gas condenser capacity it is evident that the factors mentioned above are of practical importance.

The above considerations indicate the flexibility of the new method. In addition to eliminating the involved condenser calibration, it provides a means for studying the effect of disturbing factors. The ability to make measurements over a range of frequencies without changing any of the apparatus is also an advantage in determining the complete dielectric behavior of a substance.

Before leaving the discussion of (22), brief mention should be made of the approximations involved in its derivation. The first approximation came when f_{12} in (7) was replaced by f_{11} to obtain (8). It can be very easily shown that the error involved by this approximation can be neglected. The same sort of approximation was made in obtaining (16), and since (16) and (10) enter into (22) as a difference, even these errors tend to cancel.

The second approximation came when C_{21} in (20) was replaced by C_{22} to give (21). This enters only once into the final equation and becomes of increasing importance when measurements are made at high densities and on substances of large dielectric effect. When measuring a nonpolar gas such as

nitrogen with a maximum pressure of 7 atmospheres the error in the value of $\epsilon-1$ is less than 0.1 percent. Even under less favorable conditions this accuracy can be attained by correcting (22) with an approximate value for ϵ. So (22) may be considered valid to a precision better than that of the measurements.

Description of the Apparatus

The apparatus used in the actual application of this method must be very carefully chosen in spite of the simplified procedure. Since the dielectric effect is calculated from the frequency changes of a tube oscillator, it is essential that this oscillator have a frequency stability of the highest order. It must change its frequency accurately in response to changes in capacity, but must be free from frequency shifts due to other unavoidable disturbances. It should be pointed out that this requirement must be fulfilled if accurate results are to be obtained whatever method of measurement is used. Many earlier workers appear to have neglected this point, while others have attempted to correct their results for oscillator drift. The ideal oscillator is one in which frequency drift has been eliminated, and so a very careful study was made of oscillator steadiness. The most important results of this study have already been published.[3]

The osciliator as originally described was still further improved by the addition of a temperature control. A small electric fan was arranged to blow air into the box containing the oscillator, all of the air being passed over an electric heater. By automatically controlling the heater current a very constant oscillator temperature was obtained. The control device consisted of a thermocouple, with one junction inside the oscillator box, connected to a low resistance reflection galvanometer. The galvanometer reflected a spot of light into a photoelectric cell which was connected to a thyratron relay tube in a phase control circuit.[4] The heater was placed in the plate circuit of the thyratron. This type of control was required since it was impossible to introduce a make and break circuit into the oscillator box without causing sudden changes in frequency. With this arrangement the control circuit always remained closed and did not react on the oscillator. The operation was very satisfactory, the temperature variations being less than 0.05 degree.

The beat note steadiness was further improved by placing the crystal in the thermostated oscillator box. The crystal and holder were placed in a heavy copper cylinder, to shield them from the direct blast from the fan. With this arrangement the fluctuations in the crystal temperature were very small indeed.

These refinements reduced the fluctuations in the beat note frequency to random variations of less than one cycle when the tube oscillator was operating in the neighborhood of 1,000 kc. Steady drift was completely eliminated. Rather large frequency changes occurred when the load on the commercial power lines was changed. These disturbances could not be controlled, but

[3] C. W. Miller and H. L. Andrews, Rev. Sci. Inst. **1**, 267 (1930).
[4] A. W. Hull, Gen. Elec. Rev. **32**, 213 (1929) and **32**, 390 (1929).

their effect was so great that observations made under these conditions could be easily detected.

The design of a condenser and mounting suitable for dielectric constant measurement also requires very careful consideration. The condenser and mounting shown in Fig. 3 were finally chosen after several designs had yielded inconsistent results. The condenser, a radio receiving condenser with semicircular plates, proved more satisfactory than the more modern condensers of the "low loss" type. This was due to its more highly symmetrical construction. The original hard rubber insulation was replaced with the fused quartz bushings shown in the figure. These bushings were located at equal distances

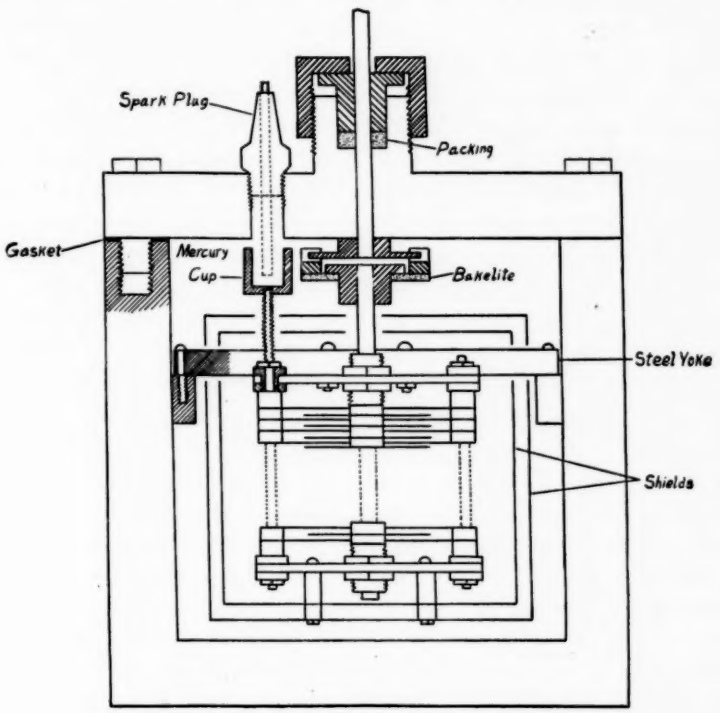

Fig. 3. Construction and mounting of the gas condenser.

from the shaft, and were also symmetrical at either end of the condenser. With this type of insulation any deformation due to hydrostatic pressure merely alters the pressure on the quartz and does not change the relative positions of the two sets of plates, even though the plates themselves undergo a slight change in all dimensions. With the asymmetric construction found in most radio condensers the deformations due to gas pressure change the spacing of the plates so that the resulting capacity change is not due to the gas alone.

It is also essential that only one part of the condenser be rigidly attached to the container. If more than one part is fastened rigidly, the deformation of the container itself will set up strains in the condenser. The most satisfactory

mounting consisted of a steel yoke fastened to the top frame of the condenser, the yoke in turn being bolted to lugs welded to the inner surface of the container.

When measurements were being made it was necessary to have the external shaft entirely free from the condenser to avoid a second point of contact. This was accomplished by the device shown in the diagram. A steel collar carrying a bakelite ring was fastened to the condenser shaft. A steel ring with diametrically opposite slots was bolted to the bakelite. A steel rod which was attached to the external shaft to form an inverted *T* fitted loosely in the slots. The steel ring was completely insulated and had a brush rubbing on its outer surface, the external connection being made through a second spark plug not shown in the diagram. When the external shaft was turning the condenser, the head of the *T* pressed against the sides of the slot and completed an electrical circuit. A dry cell and a miniature electric light formed the external indicator. A slight backward turn placed the *T* head in the center of the slot and left the condenser with only one point rigidly attached. When the circuit was broken, the light was extinguished and the condenser was known to be free.

The use of a metal container introduced another source of capacity change due to distortion. A change in pressure slightly deformed the outer container and so changed the stray capacity between the fixed insulated plates and the container itself. To avoid this, a double sheet steel shield was placed around the entire condenser. These shields were securely bolted to the lower frame of the condenser only, and so introduced no distortion. When pressure was applied the deformation of the shields was negligible since the pressure was applied to both sides. Thus the capacity between the fixed plates and the grounded shields remained unchanged. Deformation of the container produced no effect since this was at the potential of the shields.

The container formed one connection to the condenser, the other being made through the spark plug shown in the diagram. These spark plugs proved very satisfactory, being pressure tight and also having a low R.F. resistance. A brass extension on the spark plug electrode dipped into a brass cup containing mercury. This gave an electrical connection to the fixed plates, but since no mechanical forces could be transmitted through the mercury, deformation of the condenser was avoided.

The body of the container and the top were each made of a single casting. The joint between the top and the body of the container was made tight by a gasket of "Vellumoid." This was applied without shellac or similar substance to avoid contamination. The connections between the pressure chamber and the gauge, storage tanks, etc. were made through 3/16 inch steel tubing. A 1/10 degree thermometer held in the pressure chamber through a pressure tight joint of marine glue served to determine the gas temperature. In order to keep the temperature constant, the casting was immersed in a kerosene bath equipped with a temperature control. The temperature of the bath was kept constant to 0.2 degree and the fluctuations inside should be much less than this.

Gas pressures greater than atmospheric were measured with a mercury column. This consisted of a glass tube fastened to a brass mm scale, the lower end of the tube dipping in the mercury reservoir. With this arrangement any pressure below seven atmospheres could be estimated to 1/10 mm. Pressures below atmospheric were measured with a small McLeod gauge.

Two pieces of electrical apparatus were of unique design and deserve particular mention. This method requires a calibrated audio-oscillator which can be rapidly and accurately adjusted to any desired audio-frequency. These requirements eliminate the ordinary tube oscillator which requires large coils and condensers to obtain the low frequencies. The adjustment of an oscillator of this type to a desired frequency is rather laborious and the calibration is involved and uncertain.

The vibrating wire oscillator previously described[3] eliminated all of these difficulties. Only a single control was required to cover the entire range and settings could be made to 0.1 cycle. The calibration was extremely simple and was surprisingly independent of variations in temperature, amplitude of vibration, and other disturbing factors. The fundamental frequency of the wire could be varied from 250 to 450 cycles. The output, although not exactly sinusoidal, was sufficiently pure so that oscillograph figures of 9 to 1 ratio could be readily identified. This oscillator can thus be used to measure any audio-frequency between 28 and 4000 cycles.

This oscillator could be calibrated in terms of the crystal frequency by the use of a subharmonic oscillator.[3,5] This gave the value of the dielectric constant in terms of one standard of frequency. The subharmonic oscillator was also used to determine the absolute frequency of the crystal, the output of the subharmonic oscillator being used to drive a General Radio synchro-clock. With the absolute crystal frequency known, and with all audio-frequencies measured in terms of the crystal standard, any determination of the dielectric constant becomes an absolute determination, without reference to capacity standards.

Experimental Procedure

The apparatus described above has been used to measure the dielectric constant of nitrogen at room temperature at pressures up to seven atmospheres.

	Percent by weight
Carbon dioxide	0.0002
Hydrocarbons	0.00002
Hydrogen	0.00002
Carbon	0.00012
Oxygen	less than 0.5
Neon and helium	infinitesimal traces
Water vapor	less than 0.02 at 2000 pounds pressure

[5] W. A. Marrison, Proc. I. R. E. **17**, 1103 (1929).

The gas used was water-pumped nitrogen obtained from the Air Reduction Sales Co. The following analysis of the gas was furnished by the company. Oxygen and water vapor are the only impurities present in an appreciable amount. The oxygen was removed by passing the gas slowly over copper shavings heated to 500–600°C. It was then stored for at least two days in a tank containing phosphorous pentoxide to remove the water vapor.

All observations were made at night to avoid disturbances due to changing load on the commercial power lines. The temperature controls were started several hours before readings were taken in order to insure temperature equilibrium. At the same time the crystal oscillator was started and the condenser chamber evacuated. A Cenco Hyvac pump reduced the pressure sufficiently in a few minutes, but the chamber was kept evacuated for several hours to insure temperature equilibrium.

After evacuation the gas condenser was adjusted to the desired setting and released from the external shaft. The capacity was then measured on a General Radio capacity bridge for reference purposes. This reading also gave a check on the a.c. resistance of the condenser and leads. The oscillator was then started and the precision condenser adjusted until the proper beat note was obtained with the desired crystal harmonic. A loosely coupled wavemeter served to identify the harmonic.

When the tube oscillator had become steady, the condenser chamber was shut off from the pump, and all auxiliary apparatus with the exception of the heater for the tube oscillator was disconnected. The audio-oscillator was then adjusted to give a recognizable Lissajous figure on the oscillograph screen. The auxiliary apparatus was again put in operation, and gas admitted slowly from the storage tank.

Upon admission of gas, the temperature in the condenser chamber rose about 1°. Several minutes were required for the heat to be absorbed by the walls of the container. When the temperature became steady the auxiliary apparatus was again disconnected and the audio-oscillator readjusted.

This procedure was repeated, each time increasing the pressure by about 50 cm of mercury, until the maximum of the pressure gauge was reached. At this point the capacity of the gas condenser was reduced until a beat note was formed with a higher harmonic. With a little care this beat note could be made less than 400 cycles. The capacity of the precision condenser was then increased until the proper beat note was formed with the original harmonic. A series of readings was then taken, the pressure being reduced in steps of about 50 cm. The vacuum reading at the end was omitted because of the length of time required for the condenser plates to come to temperature equilibrium.

When a run was completed the subharmonic oscillator was started and the wire calibrated in terms of the crystal. This completed the data required for a run.

Experimental Results

The computations are simplified if the observations are treated graphically. Eq. (10) shows that for a given condenser setting $(\epsilon-1)$ is proportional

to $(f_{A_2}-f_{A_1})$, the frequency difference upon introduction of the gas. Now for all densities so low that molecular interaction is negligible the dielectric effect $(\epsilon-1)$ will be proportional to the density. It should be emphasized that this statement is true regardless of the nature of the dielectric. But for a perfect gas the density is proportional to the pressure as long as the temperature remains constant. Nitrogen behaves practically like a perfect gas over the range of pressures and temperatures here considered. Hence, if the frequency change is plotted against pressure, a linear relation should result. Actually two linear relations will be obtained, one for each setting of the condenser. The slope of the first line, i.e., the frequency change per normal atmosphere, will be the factor $(f_{A_2}-f_{A_1})$ in (22). Similarly, the second slope will be $(f_{A_5}-f_{A_4})$.

The computations can be further simplified by noting that the audio-frequencies which appear in (22) are all small compared to the frequencies of the crystal harmonics. If the audio-frequencies are neglected (22) becomes

$$\epsilon - 1 = \left[\frac{2n_2^2}{n_2^2 - n_1^2}\right]\left[\frac{(f_{A_2} - f_{A_1}) - (f_{A_5} - f_{A_4})}{n_1 f_c}\right]. \tag{23}$$

The correction by the perfect gas law to give $(\epsilon-1)_0$ or the dielectric constant at normal temperature and pressure is

$$(\epsilon - 1)_0 = \left[\frac{2n_2^2}{n_2^2 - n_1^2}\right]\left[\frac{(f_{A_2} - f_{A_1}) - (f_{A_5} - f_{A_4})}{n_1 f_c}\right]\frac{T}{273}. \tag{24}$$

This is easy to compute and in this particular case yields results identical with those obtained from the more general form (22).

Fig. 4 shows the relations between frequency change and gas pressure obtained in four runs. The experimental conditions under which these runs were made are listed in Table I.

TABLE I.

Run	Harmonics n_1	Harmonics n_2	Capacity mmf	Gas temperature	Slopes Cycles per atmos.	
I	9	14	629	32.1	164.5	27.3
II	9	18	703	32.3	183.0	8.8
III	9	14	592	32.0	151.7	15.5
IV	9	13	566	28.3	149.3	26.1

Fig. 4 shows the strict linearity existing between the pressure and the frequency difference. The original plot, from which Fig. 4 was reproduced, was made to a large scale so that the accuracy of plotting was comparable with the accuracy of observation. It will be noticed that a few points lie so far from linearity that they are obviously not to be considered. These correspond to observations made when outside electrical disturbances were changing the frequency of the oscillator.

None of the upper curves pass through the origin. This is probably due to lack of thermal equilibrium in the container when it is evacuated. Upon

evacuation, the temperature inside the chamber is lowered. As soon as the air is removed, however, the stationary condenser plates are thermally insulated. Heat transfer, either by radiation or by conduction through the quartz insulators, will be very slow because of the small temperature differences and the low conductivity of the quartz. As soon as gas is admitted, however, the stationary plates are able to absorb heat and come to equilibrium. Thus the introduction of gas increases the size of the condenser plates in addition to its dielectric effect, and the curves would be expected to lie above the origin just as they do. For this reason no weight was given to the origin when the lines were drawn.

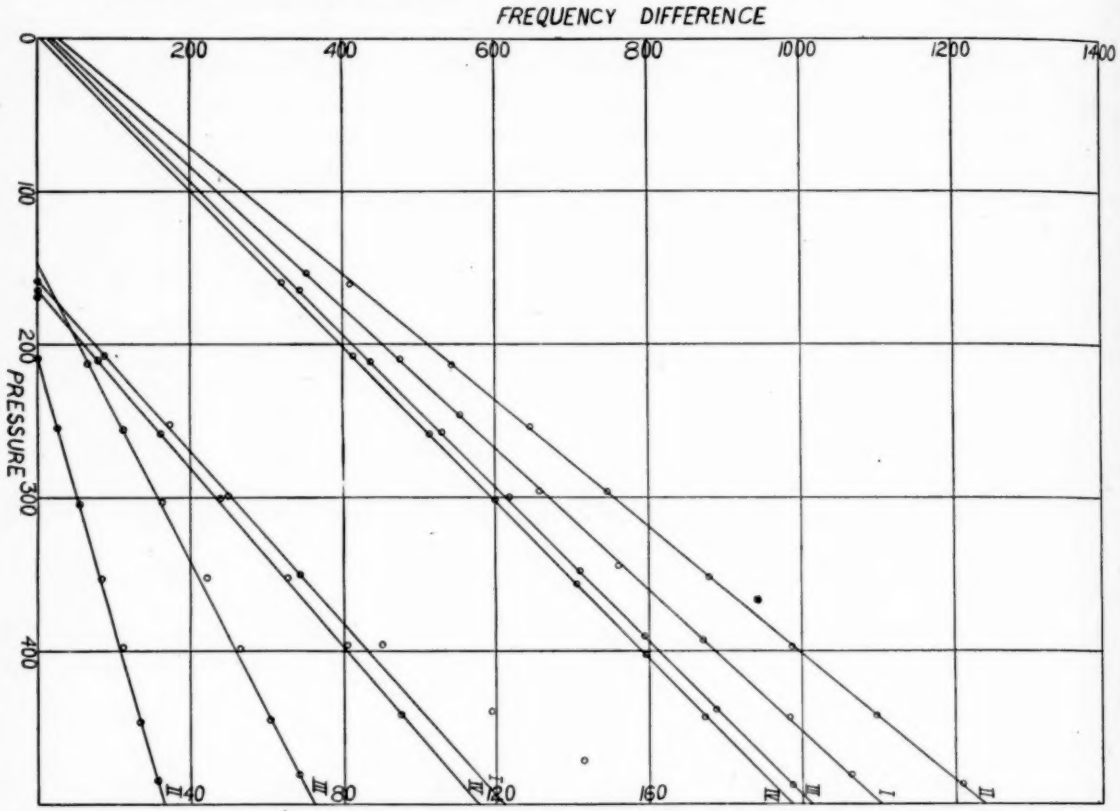

Fig. 4. Frequency change-pressure relations for nitrogen.

Discussion

The results obtained from the four runs are listed in Table II. Although these runs do not represent the full range of experimental conditions which

Table II.

Run	Harmonics	Capacity	$(\epsilon-1)_0$
I	9–14	629 mmf	0.0005914
II	9–18	703	0.0005898
III	9–14	592	0.0005877
IV	9–13	566	0.0005910

may be utilized, they are sufficient to show the applicability of the method. Since there is no evidence to show that the value of $(\epsilon-1)_0$ is a regular function of either capacity or frequency change, the above values are given equal weight. The result is an average value of $(\epsilon-1)_0=0.000589$ measured at 884 kc. From a consideration of the errors of observation and plotting, it seems that this should be correct in absolute value to better than 0.5 percent.

One of the greatest sources of error lay in the determination of the gas temperature. The behavior of the mercury-glass thermometer under pressure was rather erratic, and while it served to indicate equilibrium, did not give accurate readings. It is planned to replace this with a thermocouple.

The value of the dielectric constant obtained is in resonable agreement with other observations. The most recent refractive index measurements, carried out in this laboratory on the same sample of gas by C. E. Bennett, predict 0.000585 as the correct value of $(\epsilon-1)_0$ to an accuracy of 1 percent.[6] Probably the best previous dielectric constant determinations on nitrogen are those of Zahn[1,7] who gives 0.000580 as his final value. Since the present method eliminates the difficult condenser calibration, and gives an absolute measure of the dielectric effect over a range of experimental conditions, it is felt that the present value is the more accurate. The present data are sufficient to show the applicability of the method to a narrow experimental range. Future work will extend the range and it is hoped, increase the accuracy of the results.

In conclusion, the author wishes to acknowledge his indebtedness to Professor Carl W. Miller, who suggested the problem and gave invaluable aid throughout its development. He is also grateful to Professor A. deF. Palmer for many helpful suggestions. The major portion of this work was done while the author was a Charles A. Coffin fellow at Brown University.

[6] C. E. Bennett, Phys. Rev. **37**, 263 (1931).
[7] C. T. Zahn, Phys. Rev. **27**, 455 (1926).

CHARTS FOR TRANSMISSION LINE PROBLEMS

By H. E. Hartig

Department of Electrical Engineering, University of Minnesota

(Received October 16, 1931)

Abstract

Charts to a reduced scale are presented from which it is possible to determine with very little labor the vector voltage, current and impedance at any point of a transmission line with given terminations. Examples are given exhibiting the properties of the charts and the method of use, illustrating how without computation the variation of E, I and Z from one end of the line to the other may be visualized. The charts are chiefly useful for visualizing the electrical conditions on lines which are electrically long, that is, telephone or radio transmission lines.

AS IS well known, A. E. Kennelly has shown that the rigorous solution of the problem of steady state electrical transmission over a line with uniformly distributed constants may be expressed by means of hyperbolic functions having complex arguments.[1]

Thus for a transmission line l miles long and having per circuit mile R ohms resistance, L henrys inductance, G mhos leakance, and C farads capacity, and terminated with an impedance Z_R, the solution may be written,

$$\frac{E_R}{\sinh \delta} = \frac{E_X}{\sinh (PX + \delta)} = \frac{E_T}{\sinh (Pl + \delta)} \tag{1}$$

$$\frac{I_R}{\cosh \delta} = \frac{I_X}{\cosh (PX + \delta)} = \frac{I_T}{\cosh (Pl + \delta)} \tag{2}$$

$$\frac{Z_R}{\tanh \delta} = \frac{Z_X}{\tanh (PX + \delta)} = \frac{Z_T}{\tanh (Pl + \delta)} \tag{3}$$

where the subscript T refers to the transmitting end of the line, R to the receiving end, and X to any intermediate point. The iterative (or surge) impedance Z_K is

$$Z_K = \left(\frac{R + j\omega L}{G + j\omega C}\right)^{1/2}$$

and the propagation constant P per mile is

$$P = ((R + j\omega L)(G + j\omega C))^{1/2}$$

It is customary also to separate P into real and imaginary parts, $P = A + jB$, calling A the attenuation constant and B the wave-length constant. The complex quantity δ is defined by the equation,

[1] A. E. Kennelly, Hyperbolic Functions Applied to Electrical Engineering, 1916.

$$\tanh \delta = \frac{Z_R}{Z_K}. \tag{4}$$

The Eqs. (1), (2) and (3) giving the relations between the various electrical quantities of interest in the problem, are extremely simple being nothing more than equalities between simple ratios. Moreover, the charts of complex hyperbolic functions[2] which Kennelly has provided makes it easy to obtain theoretically correct solutions of fair accuracy. More accurate results can be obtained at the cost of somewhat greater labor by using Kennelly's tables.[3]

It would appear that nothing is left to be desired for the complete and rigorous solution of the problem.

The writer has found that students have no particular difficulty in solving specific transmission line problems, especially when using the Chart Atlas, but obtain with great difficulty or not at all a mental picture of the transmission phenomenon as a whole, a fact not to be wondered at. It is, of course, desirable that whatever is lost in accuracy by the use of graphical methods in computation, should be compensated for by a more direct or more extensive understanding of the phenomenon represented. It occurred to the writer that certain modifications would in some measure accomplish this result.

In his Chart Atlas, Kennelly graphs $\sinh (x+iq) = \rho \angle \gamma$ (for example in Chart X–XI$_A$) with ρ and γ on a uniform rectangular scale, and in consequence, x = constant and q = constant, are curved lines. The writer has constructed charts in which this procedure is inverted, that is, in the chart representing $\cosh (A+jB) = R \angle \theta$, (Fig. 2), A and B are laid off on a rectangular scale and R = constant, θ = constant, are curved lines. The consequences of this modification will be apparent when examples are studied.

The curves for $\cosh (A+jB)$ are obtained by plotting in rectangular coordinates the equations

$$\cosh 2A + \cos 2B = 2R^2, \quad R = 0.1, 0.2, \cdots$$

and

$$\tanh A \tan B = \tan \theta, \quad \theta = 10^\circ, 20^\circ, \cdots$$

where B is in circular radians and A in hyperbolic radians. The systems of curves repeat themselves at intervals of $B = \pi$ radians. Hence it is convenient to reckon B in quadrants and decimal parts thereof as is done in Fig. 2. The wave-length constant of a line when expressed in quadrants represents the length of the line in quarter wave-lengths. Hence the quadrant is a more significant and certainly a more convenient unit for this purpose than the radian.

The curves for $\sinh (A+jB)$ have the same form as the cosh curves, merely being displaced along the B axis as shown in Fig. 1. It is easy to show that the two systems of curves R = constant, θ constant, cross each other at right angles. This property makes interpolation by inspection easy. Since the curves for sinh and cosh of $A+jB$ have the same form, a single chart extend-

[2] A. E. Kennelly, Chart Atlas of Hyperbolic Functions, 1914.

[3] A. E. Kennelly, Tables of Complex Hyperbolic and Circular Functions, 1914.

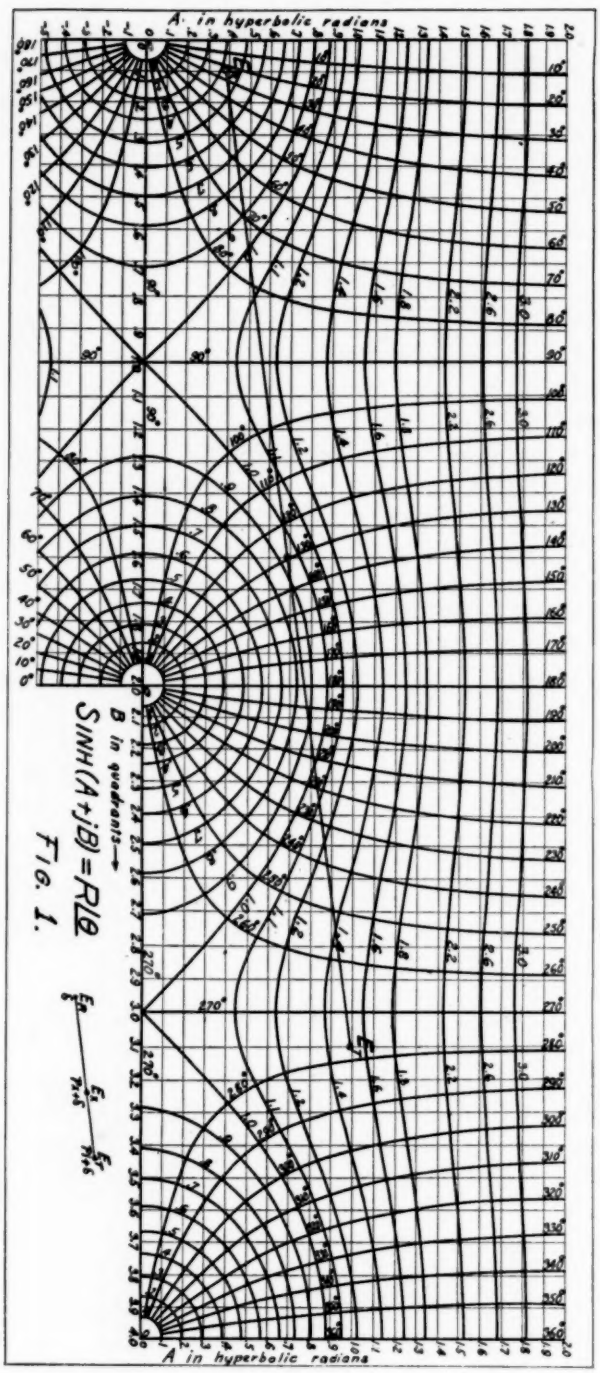
A in hyperbolic radians
B in quadrants
SINH(A+jB)=R/θ
A in hyperbolic radians

Fig. 1.

ing over two quadrants would suffice for both. They are here drawn separately and extended over four quadrants for ease of explanation.

For the chart of tanh $(A+jB)$, it is necessary to plot the equations,

$$\frac{\cosh 2A}{\cos 2B} = \frac{1+R^2}{1-R^2}, \qquad R = 0, .1, .2 \cdots$$

$$\frac{\sin 2B}{\sinh 2A} = \tan\theta, \qquad \theta = 10°, 20°, \cdots$$

These two systems of curves also cross each other at right angles as shown in Fig. 3.

The distinguishing property of these charts is that all the values required for computing E, I and Z for all the points from one end to the other of a transmission line, lie on a straight line on the charts. This follows from the fact that all the values in question are obtained from

$$PX + \delta = (A + jB)X + A' + jB' = AX + A' + j(BX + B')$$

where X takes on values from zero to l.

Since A and B are plotted in rectangular coordinates, it is clear that all of these points must lie on a straight line. Moreover, the location of these points on the charts is suggestive of the equations from which E, I and Z are obtained. This is indicated by the lines drawn in the lower right hand corners of the figures which may be compared for form with Eqs. (1) (2) and (3).

An example will make the matter clearer. Given a uniform line 200 miles long for which $P=0.003+j\ 0.015$ per mile (0.015 in quadrants) and $Z_K = 400\angle -10°$. If the voltage at the sending end is 100 volts and the load impedance is $Z_R = 1000\angle -30°$, find the voltage at the middle and end of the line. Also find the current, and the impedance looking toward the load, at the beginning, middle and end of the line.

Solution: For the given line and termination we have by Eq. (4)

$$\tanh\delta = \frac{Z_K}{Z_R} = \frac{400\angle -10°}{1000\angle -30°} = 0.40\angle 20°.$$

Referring to Fig. 3 we find for $R=0.40$, $\theta=20°$ that $A=0.386$, $B=0.100$. Since $P=0.003+j\ 0.015$, we easily obtain the following values for the end, middle and beginning, respectively.

	δ	$100\ P+\delta$	$200\ P+\delta$
A	0.386	0.686	0.986
B	0.100	1.60	3.10

These three points are shown on Figs. 1, 2 and 3, in each case connected with a straight line. The corresponding values of R and θ are then read from the curves and are tabulated below. Actually the values shown were taken from more accurately drawn charts with smaller subdivisions than those shown here.

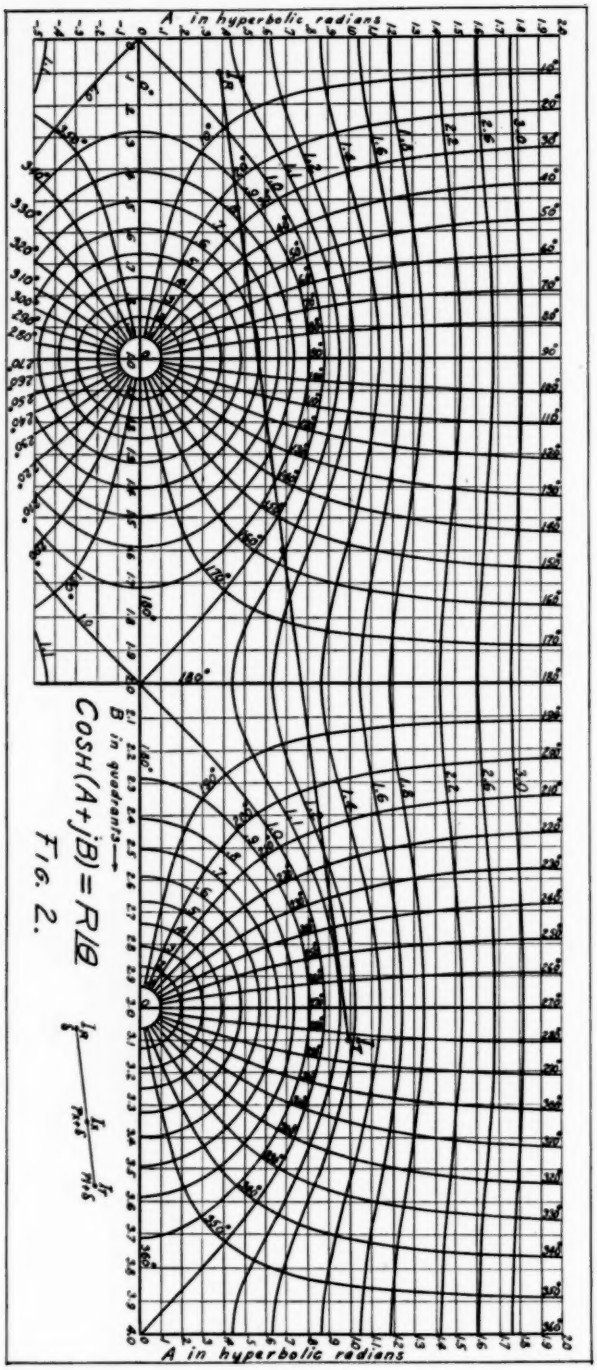
A in hyperbolic radians
B in quadrants
COSH(A+jB) = R/θ
A in hyperbolic radians

Fig. 2.

	δ	$100\,P+\delta$	$200\,P+\delta$
sinh	$0.43\ \angle 23°$	$0.94\ \angle 129°$	$1.52\angle 277°$
cosh	$1.065\angle 3.5°$	$1.095\angle 157°$	$1.16\angle 281°$
tanh	$0.40\ \angle 20°$	$0.86\ \angle -28°$	$1/.77\angle -5°$

Whence by Eq. (1), putting $E_T = 100$ volts as required, we have

$$\frac{E_R}{0.43\angle 23°} = \frac{E_{100}}{0.94\angle 129°} = \frac{100}{1.52\angle 277°},$$

or $E_R = 28.2\angle -254°$ volts and $E_{100} = 61.8\angle -148°$ volts.

The current at the end of the line can now be computed as follows,

$$I_R = \frac{E_R}{Z_R} = \frac{28.2\angle -254°}{1000\angle -30°} = 0.0282\angle -224° \text{ amperes.}$$

Then by Eq. (2),

$$\frac{0.0282\angle -224°}{1.065\angle 3.5°} = \frac{I_{100}}{1.095\angle 157°} = \frac{I_T}{1.16\angle 281°},$$

whence $I_T = 0.0307\angle 53.5°$ amperes, and $I_{100} = 0.0290\angle -70.5°$ amperes.

For the impedances we have by Eq. (3),

$$\frac{100\angle -30°}{0.40\angle 20°} = \frac{Z_{100}}{0.86\angle -28°} = \frac{Z_T}{1/0.77\angle -5°}$$

whence $Z_T = 3240\angle -55°$, and $Z_{100} = 2150\angle -78°$.

This completes the solution, but as already mentioned it is not so much in computing values for specific points on the line that the charts are useful as in giving by inspection information about the behavior of the entire line. For example, by Eq. (1), E_x must vary directly as sinh $(Px+\delta)$, hence by noting the magnitude of sinh $(Px+\delta)$ on the straight line which represents points on the transmission line, we can trace the variation in voltage from one end of the line to the other. Thus starting with the transmitting end the voltage falls steadily, the line crossing 1.4, 1.2, 1.1, 1.0, etc., until it reaches a minimum just before the middle, then it rises again until at about the $\frac{2}{3}$ point it reaches a maximum voltage of roughly $1.13/1.52 = 75$ volts after which it falls again for the remainder of the distance. The phase angle decreases with distance from the transmitting end, first slowly, faster at the minimum voltage, more slowly at the maximum voltage, and finally faster again as it approaches the receiving terminal.

In a similar manner the variation of current and impedance may be traced on Figs. 2 and 3, respectively, and perhaps unsuspected peculiarities uncovered. In the present instance the current is seen to have a larger value at the $\frac{1}{3}$ point than at the transmitting end, and at the $\frac{2}{3}$ point a smaller value than at the terminus.

If a different value of load impedance is used than the given one, the effect is merely to move the representative line on the chart parallel to itself, the left end being at the new value of δ defined by the new receiver impedance Z_R and

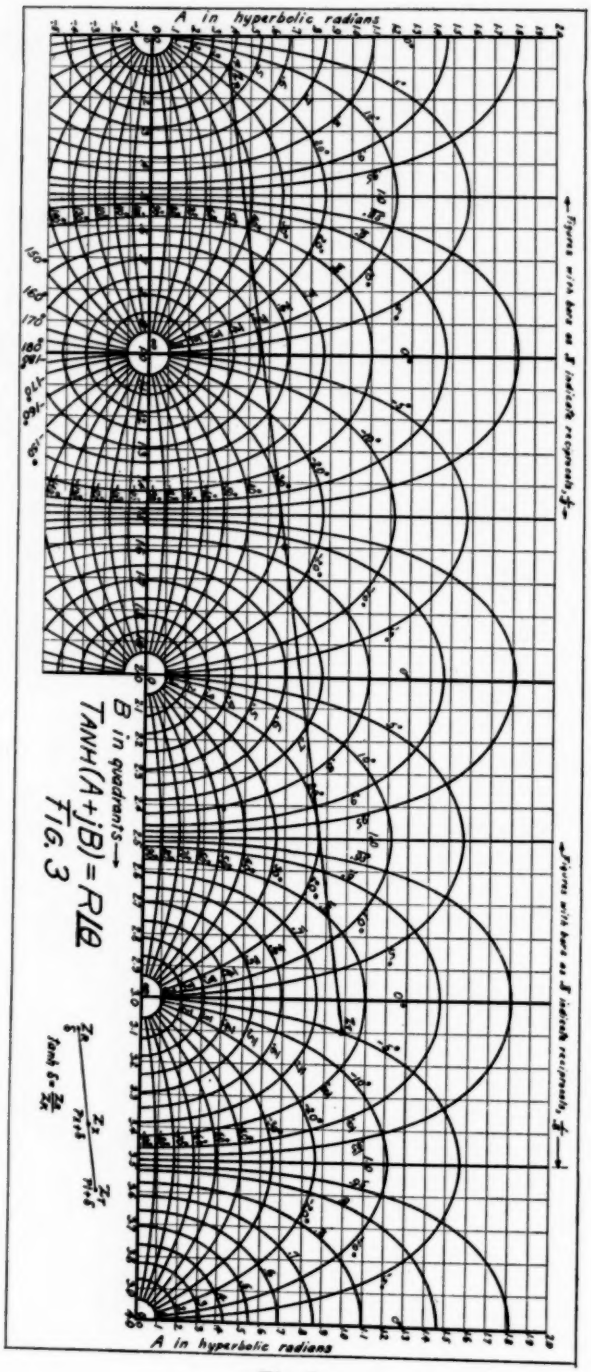
A in hyperbolic radians
B in quadrants
TANH(A+jB) = R/θ
FIG. 3
A in hyperbolic radians

Fig. 3.

the relation $\tanh \delta = Z_R/Z_K$. So that if one had to do always with the same line, or lines of similar construction but different lengths, a triangle could be constructed with the appropriate slope, $\tan B/A$, and a scale of miles laid off on the incline from left to right to serve for all the cases that could arise.

For power lines and radio transmission lines, the attenuation is usually very small and in consequence the slope of the representative line is small. By reference to the charts it will be seen at once that on such lines of sufficient length, violent periodic fluctuations in voltage and current will take place when δ has a small value of A. On the other hand, for telephone cable circuits the attenuation is relatively large so that the representative line on the chart is steep. For such lines it is evident that both voltage and current will vary without periodic maximum and minimum values.

If a line is short-circuited, then $Z_R = 0$, $\delta = 0$, and $A = 0$, $B = 0$. If the line is open at the end, $Z_R = \infty$, $\delta = \infty$, and $A = 0$, $B = 1$. By observing the position of the voltage and current lines on the charts in the two cases, it will be seen (as is well known) that the current varies in the same way when the line is shorted as does the voltage when the line is open and vice versa.

It will also be observed that when a line is open at the receiving end, the greatest voltage exists at the receiving end when the line is somewhat shorter than 1 quadrant, that is, one quarter wave-length long, although for power lines, when the attenuation is small, the difference is small. In analytical treatments this fact is rarely brought out. Erroneous statements are also frequently made in this connection whereas the facts are evident from a brief study of the charts. For telephone lines the optimum so-called Ferranti effect may be obtained for all lengths from zero to one-quarter wave-length depending upon the ratio of A to B. When this ratio is larger than unity (B in radians), the effect is not obtained at all, the voltage decreasing steadily from the transmitting end to the distant open end.

If Z_R is nearly equal to Z_K in magnitude and phase angle, that is, if the load impedance nearly matches the iterative (surge) impedance of the line, then δ will have a relatively large value of A and in consequence the representative line will lie wholly in (or beyond) those parts of the chart where R changes almost exponentially and θ almost linearly. This, of course, is the nature of the behavior of a transmission line of infinite length and is easily calculated and understood.

It is possible for δ to have negative values of A. By examining the general expression for Z_K in terms of R, L, G and C, it will be seen that the angle of Z_K may vary between the limits of plus and minus 45 degrees. Since the angle of Z_K may vary between the limits plus and minus 90 degrees, it follows that the angle of $\tanh \delta = Z_R/Z_K$ may vary between the limits of plus and minus 135°. This allows, as will be seen on Fig. 3, for negative values of A restricted to about $A = -0.4$. It might be thought possible for the representative line to pass through the point $A = 0$, $B = 1$, or $A = 0$, $B = 2$. If this were possible, infinite currents or voltages might exist on the line. However, the value of δ and the slope of the line both depend upon R, L, G and C and in such a way that unless both R and G are zero the representative line cannot pass through the points in question, although it may approach very near.

Without illustrating the matter any further, it will perhaps be understood how information may be obtained from the charts for other than the conditions assumed here.

A "MAGNETIC SHARPENER"

By L. W. McKeehan

Yale University

(Received November 4, 1931)

Abstract

The claim that the mere placing of a double-edged safety razor blade upon the poles of a specially designed permanent magnet has a sharpening action has been investigated by studying the characteristics of the device and by testing the sharpness of blades so treated in comparison with untreated and with mechanically stropped blades. No definite "magnetic sharpening" was observed to occur in these tests.

Introduction

AT SEVERAL times during the past year my attention has been drawn to advertisements of a so-called magnetic sharpener for safety razor blades of the double-edged type, and I have been asked whether the device operates as claimed. In order to resolve my own uncertainty I bought one of these devices and have made a few tests upon it. After some hesitation I have decided to publish my findings, incomplete as they are, because they suggest to me that the advertisements are misleading and that they can only damage the reputation of physics as applied to every-day uses.

Characteristics of the Device

Figure 1 shows at the left three views of the device, which consists essentially of a U-shaped magnet in a molded container. At the top is a plan with the hinged cover removed and a blade in position. Below this are side and end elevations, half in section, showing among other details a spring attached to the cover. Four projecting leaves of this spring bear upon the upper surface of the blade, not shown in these views, when the cover is closed. A spring latch opposite the hinge holds the cover down against the action of this spring. The magnet, shown black in section, has its pole faces ground at an angle of about 7° to the base of the container. The sketches at the right show, much enlarged, the relation of one sloping pole face to a razor blade (A and B) and to a thicker strip (C) of soft steel— a "keeper"— furnished by the manufacturer.

When a blade is laid in position its ground edges are substantially in contact with the smooth-ground pole faces, as at A, and the sharpening action is said to depend upon the precision of this fit. If the blade while in this position were to be slid in the direction of its length a setting and honing effect would be anticipated, but such sliding is not specified for double-edged blades. The magnet is actually harder than razor steel, as claimed, so that a razor edge should be straightened or "set" by merely pressing it firmly enough against the pole. However, when the cover is completely shut the blade is bent and

the edge itself rises from the pole face, as at *B*. This takes place with a blade of the form shown in Fig. 1 and *a fortiori* for blades of more recent design with more of the central portion cut away.

The amount of the bending just mentioned was determined directly by allowing a small pool of plaster-of-paris to set upon the central portion of a blade while the cover was shut and then bending the blade, with the cover open, by direct loading at the points of contact of the cover-spring, until the plaster-of-paris casting again fitted against the blade surface. The total force exerted on the blade by the cover turned out to be about one kilogram.

Since the cover-pressure is not so applied as to increase the intimacy of contact it is only necessary to estimate the pressure due to magnetic attrac-

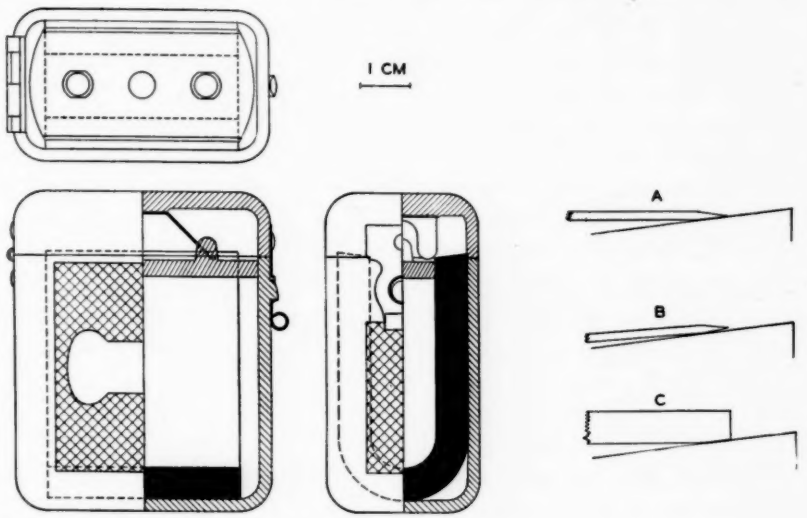

Fig. 1.

tion. This pressure is claimed to be that effective in sharpening. In order to find out what it might amount to under the best conditions I first ground the edges of the keeper, as shown at *C*, so as to fit the magnet as well as possible over a total area about equal to the beveled area of a razor blade, fitted it with screw eyes for attaching a lifting tackle, and measured the pull required to separate keeper and magnet. Since the necessary pull is diminished by any dissymmetry we may take the maximum pull to separate as most nearly the value for the static attraction. The maximum pull so found was about 5 kilograms, indicating excellent magnetic quality in a magnet weighing only 187 grams. This test also showed that the magnet here examined was at least of average quality since the maker only claims this pull to be "over seven pounds." A pull of 5 kilograms corresponds to $\overline{B^2} = 2.4(10)^8$ or, say, r.m.s. $B = 1.55(10)^4$, a not unreasonable value for a magnetic joint of this sort.

The static attraction between the magnet and a razor blade cannot be found in the same manner, for the blade is too flexible to pull away without bending. We may estimate it, however, by comparing the total magnetic fluxes through armature and blade when consecutively placed in contact with

the magnet. By a ballistic method I found $\Phi_{blade}/\Phi_{armature}=0.29$, and if we assume similar flux distributions over the contact areas for an admittedly rough approximation this gives for the attraction on a blade $5(0.29)^2=0.4$ kilogram, or less than half the maximum cover-pressure. Such a pressure is very easily exerted by one finger and is less than the pressure usually applied in stropping a blade.

Sharpness Measurements

Since neither mechanical nor magnetic pressure appeared probably adequate as a sharpening agent I decided to measure the sharpness of a few blades before and after the so-called magnetic sharpening process to see whether, in fact, they were sharpened thereby to any notable extent. The method I chose for measuring sharpness was that described by Honda and Takahasi.[1] The blade, mounted vertically in a brass block with the cutting edge horizontal, was drawn slowly to and fro across a stack of paper strips clamped down on a metal bed. Guides and stops prevented rocking or bending of the blade and limited the constant length of the stroke so that the corners of the blade did not act as ploughs. The paper chosen was a good grade of condenser paper about 0.0013 cm thick, and the stack, containing several hundred strips, was moved after each stage of the test so that the first stroke of each set was always made on an unbroken stack of full thickness. The number of sheets cut through in a standard number of strokes measures the sharpness, and the cutting of the paper itself dulls the edge gradually. While conditions as to service are rather different from those met with in shaving, I think that any true sharpening action should be apparent in the results.

In the first series of tests four different makes of blade were tested in pairs. All blades were tested immediately after unwrapping. One member of each pair was placed in the magnetic sharpener at intervals and the other was not. The total number of sheets cut was not recorded, but the number cut in four strokes was frequently counted and this datum is plotted in Fig. 2 against the number of the terminal stroke. The full line in each case connects points for a blade magnetically sharpened before each four-stroke test, the broken line to a blade not sharpened in any manner.

As a matter of interest to shavers it may be stated that an ordinate of 10 or less in Fig. 2 corresponds to what shavers call a dull blade. The sharpest blade in these tests is almost too sharp for safety.

While the results did not indicate any very conspicuous sharpening as a result of the recommended procedure the results may have been vitiated by the fact that the blade selected for "sharpening" was in each case the sharper of the two. It might be argued that these initially sharper blades are in some way defective and so fail to respond to a treatment beneficial to blades of average quality.

In the second series of tests three new blades of make *A* were used in rotation, one being untreated throughout the tests, one being sharpened magnetically, and one being sharpened by a stropping machine. In order to make

[1] K. Honda, K. Takahasi, Sci. Rep. Tohoku Imp. Univ. [1] **16**, 755–773 (1927).

results more nearly comparable both edges of each blade were tested and the direction of the first stroke in each test was systematically varied. The magnetic treatment was given to both sides of the second blade, the time with cover closed being about the same in every instance. The stropping machine was also used as nearly as possible in the same way at each step.

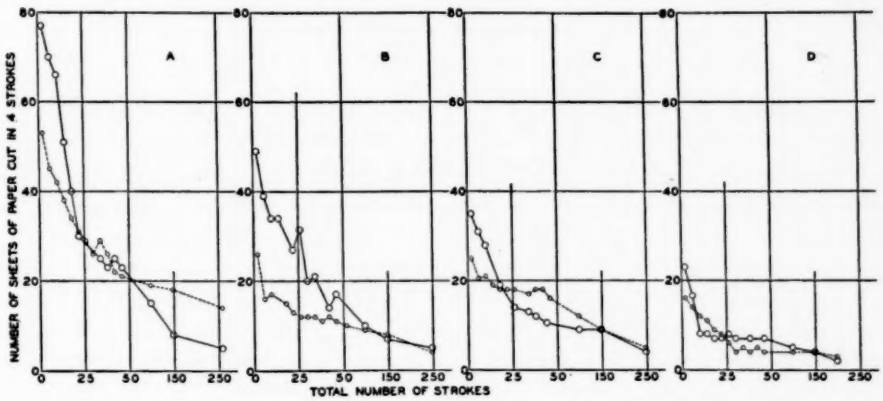

Fig. 2.

The results are presented in Fig. 3. Here the whole number of sheets cut, up to the end of each cycle of operations, has been plotted for each of the six edges concerned. The abscissa is again the number of the terminal stroke. The

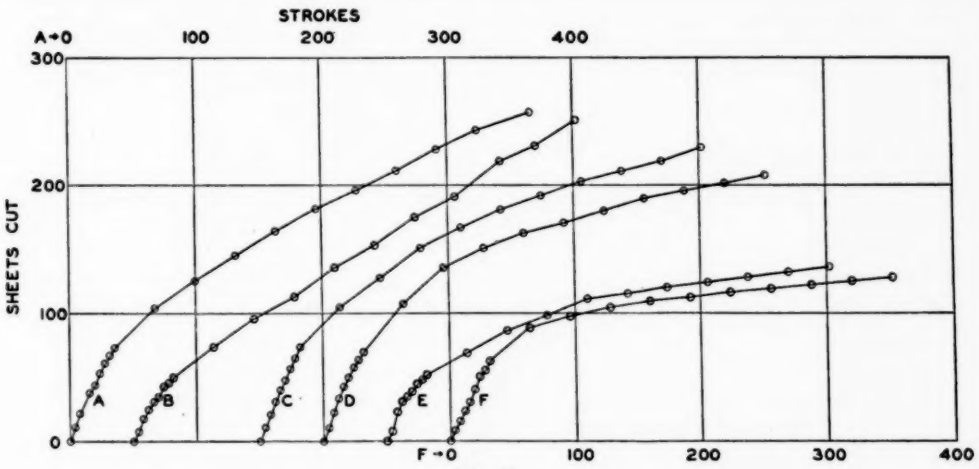

Fig. 3.

chance of accidental damage at any stage is the same for each edge, since all were handled similarly, except for the intentional differences, and no accidents are known to have occurred. The mechanically stropped edges are *A* and *B*; the magnetically treated edges are *D* and *E*; the untreated edges are *C* and *F*.

Again there is no positive evidence of magnetic sharpening unless the change in slope near the beginning on line *E* is to be so interpreted. There is

positive evidence that mechanical stropping helps in maintaining a fair degree of sharpness. It should be noted that the load on the edge and the length of stroke were different in this series from the corresponding variables in the first series, so that direct comparisons between the two series are impossible. At the conclusion of the second series, however, edges E and F at least were definitely too dull for use, while A, B, and possibly C were in serviceable condition.

Discussion of Results

A conspicuous feature of these data is the wide difference which may exist between the properties of edges intended by the manufacturers to be alike, e.g. the two edges of a single blade. This makes generalization from a few cases particularly dangerous, but I think I am justified nevertheless in concluding that the effect of treatment in the magnetic sharpener is less beneficial than the advertiser claims in such phrases as these:

"An instantaneous, automatic sharpener, in which a powerful magnet takes the place of all stropping, honing or crank-turning,"—"the strong magnet of the amazing Sharpener *instantly* draws the bent "teeth" into straight and true alignment—restoring factory keenness *absolutely*".

Extravagant statements like these, if untrue, can only diminish the confidence of the general public in better-founded claims presented for inventions in which physical principles are correctly applied.

It is a pleasure to express my indebtedness to my assistant, Mr. L. H. Ott, who constructed the sharpness tester and carried out the first series of measurements therewith.

THIXOTROPY OF LITHARGE AND GLYCERINE[1]

By E. Karrer and P. Wasserman
Medical School, Western Reserve University, Cleveland, Ohio

(Received October 16, 1931)

Abstract

Thixotropy may be defined as change in viscosity; or as change in the hardness of the solid state, after mechanical agitation. Rate of hardening decreases with increase of glycerine (critical point near 32 percent). Rate of hardening increases with rise of temperature. Water accelerates rate of hardening. Acids increase, bases decrease rate of hardening in general. Samples of litharge and of glycerine vary greatly because of differences in particle size, in composition, and particularly amount of moisture.

I. Introduction

A MIXTURE of litharge and glycerine will thicken on standing, but will become thin again when shaken. Even when the mixture stands long enough so that it becomes a brittle solid, it may still be transformed from this solid state into a very soft state by vigorous shaking. When the viscosity of a rubber solution is measured for different pressures, it is found that it decreases with increase of pressure. The flowing of such a sol is easier the faster the flow. The Poiseuille relation of viscosity to pressure does not hold. Recently[2] this phenomenon of change of viscosity with agitation has been christened with the name *thixotropy*.

The purpose of this paper is to point out the thixotropic transformation in a mixture of litharge and glycerine. This mixture constitutes a cement with many uses from the plumber's trade, where joints are sealed with it, to the paper industry where pulp tanks have been lined with it. The thixotropic nature was discovered while employing it as an electric insulator and as a shield against x-rays.

One inducement for investigating this cement was the fact that it constituted in several ways a very good analogy of the rubber system and further appeared to be such a marked example of thixotropic systems with simple elements. This is the only system in which the thixotropic property has been observed as such in detail in both liquid and solid states.

This system also affords a good illustration of an autocatalytic reaction in which the mechanism is quite clear. Water very greatly accelerates; and is formed during the reaction. The nature of the hardening curve suggests an autocatalytic reaction. The effectiveness of water to accelerate appears to be a logarithmic function and this suggests that other catalytic activity may be likewise. The reaction most probably is $C_3H_5(OH)_3+PbO=(C_3H_6O_3)Pb+H_2O+\text{heat}$.[3]

[1] Read before the Cleveland Acad. Med., Experimental Section, October 24, 1930. Abstracted, Clev. Acad. Med., Nov. (1930).

[2] Peterfi, Arch. f. Entwicklungmechanic d. organism **112**, 660 (1927).

[3] Merwin, J.I.E.C. **9**, 390 (1917).

II. Change of Viscosity with Time After Agitating

Several grades of litharge were used in these experiments: *A*, straw-colored, specific gravity 9.39; *B*, sublimed litharge, specific gravity 9.40; *C*, sublimed yellow lead, specific gravity 9.40. When heated to 105°C the change in weight of these materials was +0.039, −0.009, and +0.012 percent respectively. At incandescence the losses were 0.75, 2.18, and 0.24 respectively. The grades of litharge differ quite markedly thixotropically, and even samples of the same grade appear to vary appreciably. Specimen No. *A* required at least 32 cc to make 100 g of litharge into a thin paste; for litharge *B* it required only 20 cc; and for litharge *C*, 40 cc.

If the rate of hardening is observed when such mixtures have been prepared, it is found that *A* will have reached a durometer hardness of 90 in 35 minutes; *B* will have reached 95 in 90 minutes; and *C* will have reached 95 in 34 minutes. Other points on the hardening curve for the mixtures mentioned above are shown in Table I.

Table I.

Specimen	Time after mixing	Durometer reading	Specimen	Time after mixing	Durometer reading	Specimen	Time after mixing	Durometer reading
A	27 min.	5	*B*	47 min.	2	*C*	25 min.	3
	33	55		76	55		32	50
	35	90		90	95		34	95

The particle size and chemical composition influence the rate of reaction and therefore the rate of transformation from soft to hard state.

A typical curve representing the change of viscosity with time before and after stirring is given in Fig. 1. In this case about 20 cc glycerine were stirred into 100 g of litharge (grade *B*). The time of flow was measured through tubes with appropriate diameter, from 4 mm × 5 cm to tubes more than 1 cm in diameter and less than 1 cm long. The time is reckoned after the two ingredients have been mixed. This mixing process usually consumed about 2 minutes. There is a period in the neighborhood of 15 minutes in this case during which the viscosity changes very slightly. Thereafter, it gradually increases until about 40 minutes after mixing it attains a very high rate of change. When it is stirred at this point (*A*) the viscosity drops to a value (*B*) that is equal to that which it had at 13 minutes. On standing the process of thickening goes on to a value (*C*) several times that at the first stirring, and again after stirring drops abruptly to a low point (*D*). A recovery in the viscosity brings the value up in the neighborhood of the previous one (*E*), but this is supplanted again after stirring by a very low value (*F*). Upon standing this thickening takes place rapidly to the extremely high value (*G*) soon after which permanent hardening sets in. The rate of thickening is increased on subsequent stirrings. The drop in viscosity upon stirring becomes less and less after the system approaches a permanently hard stage. The initial period of slow hardening is shortened after subsequent stirrings. The energy necessary

for stirring becomes greater with the lapse of time after mixing. This is qualitatively indicated by the width of the cross-hatched points at *A*, *C*, *E*.

III. Thixotropy as a Change in Hardness

The changes in the consistency of such a mixture may be observed by means of a durometer even after it has hardened to a point where it will not

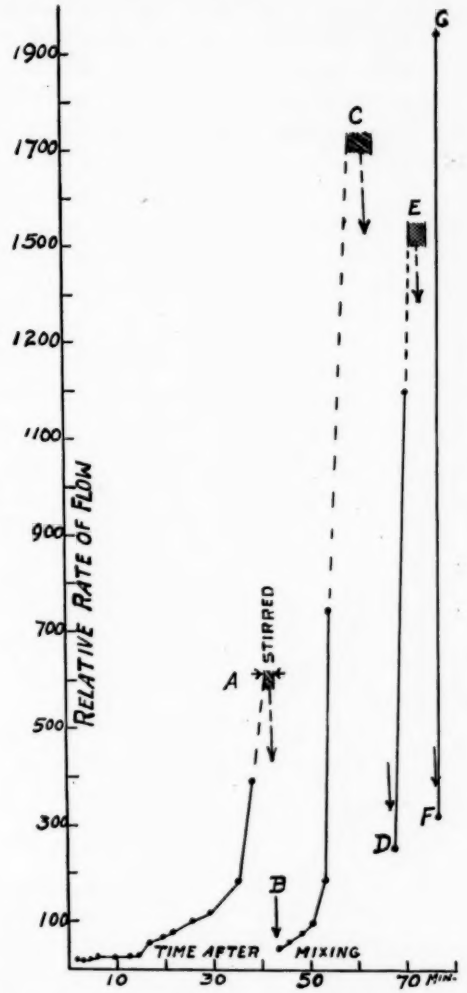

Fig. 1. The change of viscosity with time of stirring.

flow under gravity. (The Shore durometer, commonly used in the rubber industry, was employed in the present case.) The mixture may be caused to go through many cycles from liquid to solid with a hardness up to the upper limit (100) of the durometer scale. (An idea of this hardness scale may be had by noting that on the palm of a durated hand the durometer scale reading was about 30.) In all subsequent curves depicting thixotropic changes, it is variation in this durometer hardness which will be noted. The rate of the first

or any subsequent hardening depends upon the amount of glycerine used in the mixture. The minimum of glycerine which may be mixed with a given amount of litharge to yield a paste of uniform consistency in the present instance, is not much less than 2 cc of glycerine to 10 g of litharge. This ratio will depend upon the dryness and nature of the glycerine, upon the dryness and physical and chemical condition of the litharge, and upon the temperature at which they are mixed. With a previous sample good pastes were obtained with 1.5 cc. There is likewise a limit to the amount of glycerine which may be stirred into a given amount of litharge to yield the maximum hardness. When more than this amount is used the mixture, although it will stay hardened, will attain a lower hardness limit. For the present litharge and glycerine, this upper limit was in the neighborhood of 30 cc of glycerine to 50 g of litharge.

In Fig. 2 is a series of curves showing the effect of different amounts of glycerine when mixed with litharge at room temperature. Not much less than 15 cc could be mixed with 50 g litharge and yet obtain a homogeneous paste.

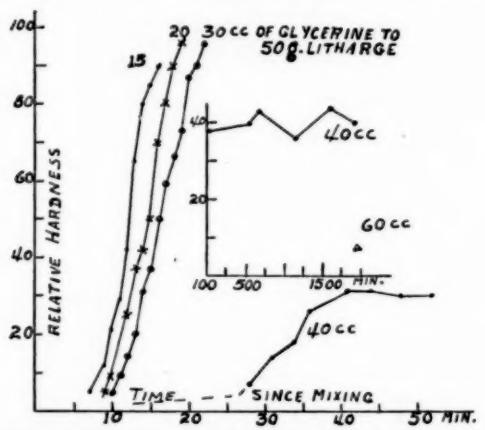

Fig. 2. The change of relative hardness after stirring. The effect of concentration of glycerine.

The rate of hardening is quite rapid and somewhat of a sigmoid form. The initial or induction period is also quite short. For 20 and 30 cc of glycerine the rate of hardening becomes slightly less and the induction period slightly longer. For 40 cc the induction period is greatly increased—there being only a small increase in hardness even in 25 minutes after mixing. Thereafter, however, the rate becomes considerably greater, but appreciably less than the rate with the other amounts of glycerine. Also in this case we note that the final maximum hardness is very much lower than that in the previous cases. This hardness was followed for many hours, as shown in the insert, without any appreciable increase over that which had been attained within 45 minutes. With 60 cc of glycerine the changes in characteristics are very greatly enhanced (see insert, Fig. 2.). There is no appreciable hardening until about 33 hours have passed. This low hardness appears also to be the maximum hardness attainable by this mixture,—no increase having been noted even days after these observations were ended.

The difference in the rate of hardening and in the induction period and in the maximum hardness attained was so great between 30 and 40 cc that a few supplementary curves are given in Fig. 3 for the intermediate concentrations of 30, 32, 36, and 38 cc of glyerine. These form a series consistent with those

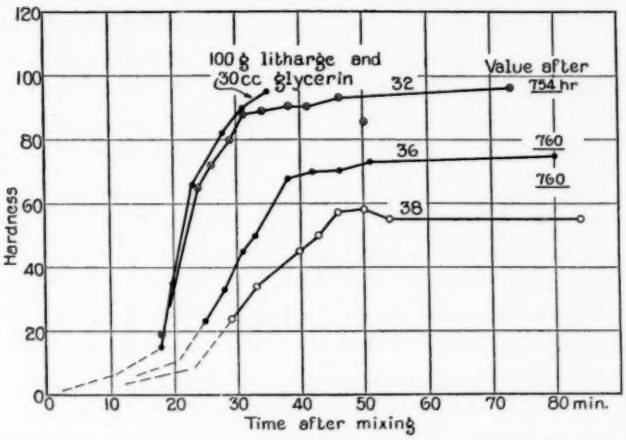

Fig. 3. The change of hardness after stirring. Effect of concentration of glycerine in the critical region near 32.7 volume percent.

just described, the induction period becoming greater, the rate of hardening and the final maximum hardness becoming less as the amount of glycerine is

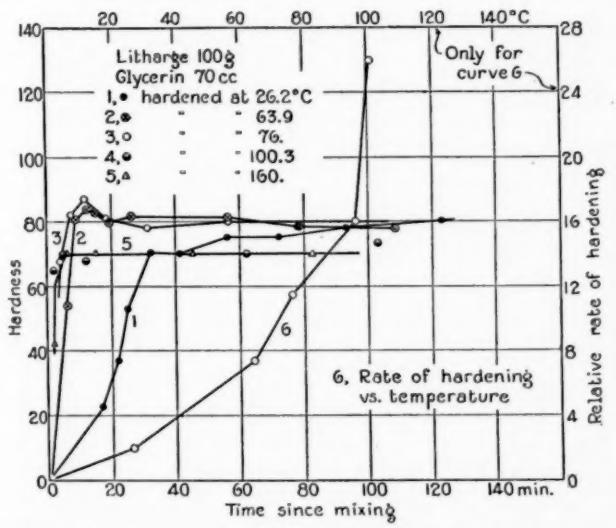

Fig. 4. The change of hardness with time after stirring at several temperatures between 26° and 160°C. Curve 6—Change of rate of hardening with temperature.

increased. It does appear, however, that in the neighborhood of 32 cc of glycerine to 100 g of litharge is a critical region, so far as the induction period and the rate of hardening and the decrease of final hardness are concerned. This indicates that the reaction involves equal numbers of molecules of gly-

cerine and litharge possibly to form ($C_3H_6O_2$) PbO as Merwin suggests (C. A. 11, 1748).[2]

IV. Effects of Temperature

The rate of hardening of a mixture of glycerine and litharge changes very rapidly with the temperature as is common in chemical reactions. A series of observations illustrating this is given in Fig. 4, for a mixture of 70 cc of glycerine in 100 g of litharge. The final hardness attained is almost, if not quite, independent of the temperature at which the mixture was allowed to harden. The mixture at room temperature attained practically its maximum hardness in about 55 minutes; at 63.9°C, this time was reduced to 9 minutes; at 76° to 7 minutes; at 103° to 2.5 minutes; at 150° in a time also of this order, but being too short to measure accurately. There is an indication of what one might term "over shooting" in hardness in several of the curves. Such an effect was observed on several other occasions when mixtures where allowed to harden at room temperature, but then the decrease in hardness was usually after longer intervals of time and may have been attributable to diffusion of glycerine or water to the surface. There also are indications that when hardening takes place at the very high temperature, the ultimate hardness is not as great as in the case of low temperature hardening. It appears that the structure responsible for the final hardening has not time for formation when the speed of hardening is too great. This softer product obtained at high temperature may also be a result of hydration, if water is eliminated during the reaction. These cements even when very hard may be made crumbly by prolonged immersion in hot water.

The chemical reaction involving some sort or combination of litharge and glycerine takes place independently of the formation of the structure in the system. Evidence for this lies also in the fact that the mixture cannot be kept liquid indefinitely by stirring. Even when vigorously stirred the mixture does harden, and presumably, if stirring were vigorous enough, the final condition would be that of a powder containing the particles approaching molecular size of litharge and glycerine in chemical combination.

For a clearer indication of the effect of temperature the rate of hardening in the region where it is more or less linear may be plotted against temperature, as it is shown in curve 6 (large circles) of Fig. 2. The rate of change with temperature increases 3.6 times from 26.2° to 63.9°; 1.6 times from 63.9° to 76°; 2.4 times from 76° to 100.3°. These high rates of changes in speed of hardening are to be expected, if the reaction is a chemical one, and if formation of the structure determining hardness proceeds at a speed equal to or greater than the speed of the chemical reaction.

V. Effect of Water

Many observations had been made before it was found that water has a profound influence upon the rate of hardening. This is shown in a particular batch of glycerine and litharge in Fig. 5, where in one instance there was added 12 percent of water on the volume of glycerine and in the other no water.

The effect of water is to shorten the period of induction and to increase the rate of hardening both before and after stirring. This effect is shown in greater detail in Fig. 6, where curves are given to show the change of hardness with

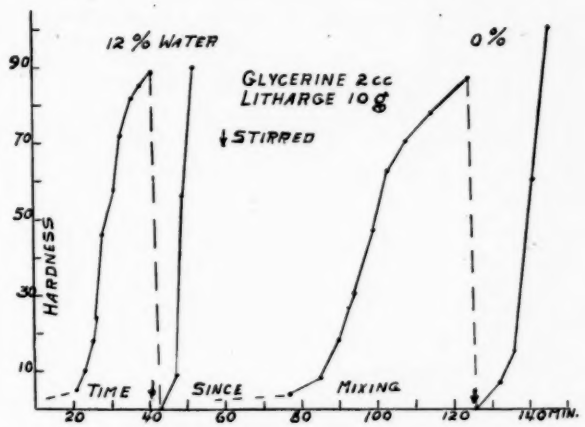

Fig. 5. The change of hardness with time after stirring with 12 percent and 0 percent of water in the glycerine.

time after various amounts of water from zero to 54.5 percent were added. The first small additions of water up to 1.6 percent affect the viscosity relatively more than subsequent additions of water.

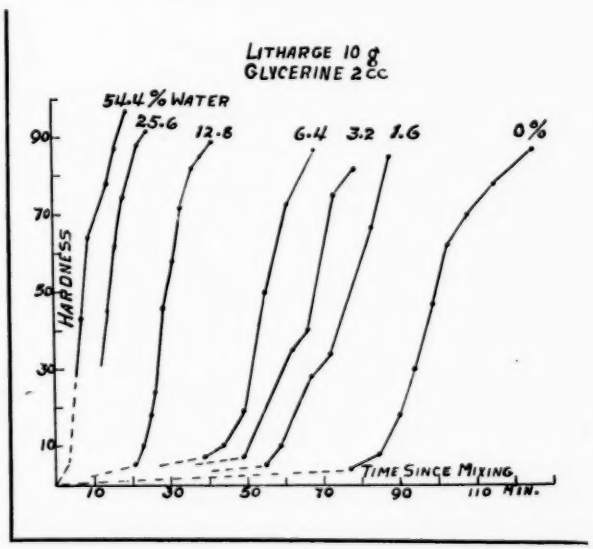

Fig. 6. Change of hardness with time after stirring for several different amounts of water in the glycerine.

The nature of this change is better brought out by the curves of Fig. 7, where the time required to attain to a hardness of 40 is plotted against the amount of water added in volume percent on the glycerine. The effect on both

the first hardening and that after the first stirring subsequent to mixing is given in the two curves. The increase in the rate of hardening is very rapid for the first 5 or 6 percent of water,—approaching an asymptotic value for 35 or more percent of water. More details of the effect of water absorbed by the glycerine and litharge as purchased will be given later.

VI. Effects of Various Liquids

Effects of acids were observed by putting two drops into the same litharge and glycerine mixture used above. The data are shown in Table II.

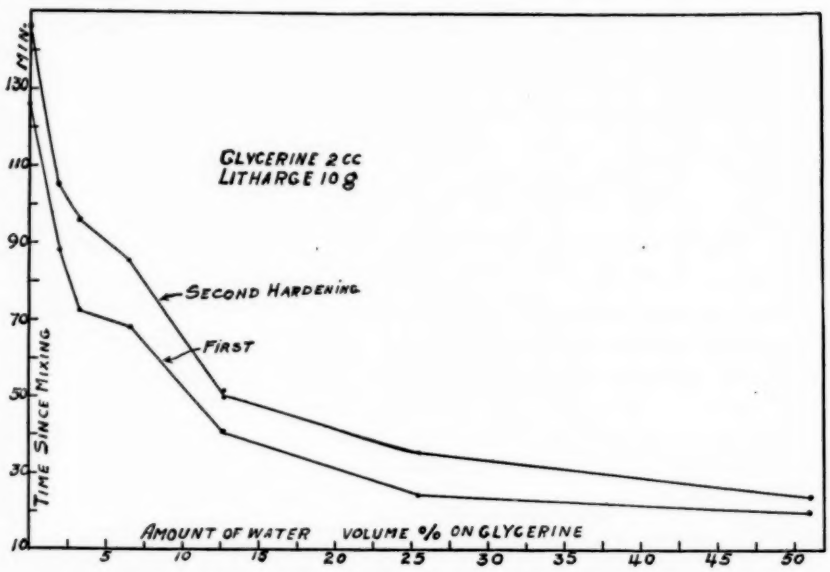

Fig. 7. The change of time required for hardening up to a durometer hardness of 40 with the amount of water in the glycerine.

The effect of bases was observed by mixing in the base litharge-glycerine mixture (0.1 grams) of the substance. (see Table III).

To compare with this, the effect of adding 2 drops of NaOH in a 20 percent water solution was observed. (Table IV).

Although, in general, it may be said that acids increase the time required for the first hardening and for the irreversible hardening; while bases on the other hand, in general, decrease the time required for the first hardening; there appear in these preliminary experiments to be some exceptions, and individualistic actions of some substances. In case of the bases the cations are arrayed in order of effectiveness in hastening hardening as follows: Na, NH_4, K, Ba, Fe. This effect of acids and bases is very similar to that observed in detail by Freundlich[4] in case of iron oxide sols. It was found later that the batch of litharge used for these observations was extremely nonhomogeneous.

[4] Freundlich, Kolloid Z. **46,** 289 (1928).

TABLE II.

Material	Hardening	Time between hardenings	Time since mixing	Comments
Formic acid	1st	26	26	The mixture for this acid stiffened while stirring in the acid. It remained pasty on stirring; hardened some after 12 hrs. but crumbled on stirring, and had a soft texture.
	2nd	12	38	
	3rd	9	47	
	4th	6	53	
	5th	4	57	
Lactic acid	1st	89	89	
	2nd	17	106	
	3rd	11	117	
	4th	7	124	
	5th	5	129	
	6th	2	131	
	7th	2	133	
	8th	2	135	
	9th	1	136	
Acetic acid	1st	40	40	
	2nd	14	54	
	3rd	9	63	
	4th	8	71	
	5th	4	75	
Phosphoric acid	1st	61	61	The mixture stiffened also slightly when the phosphoric acid was stirred in.
	2nd	35	96	
	3rd	13	109	
	4th	11	120	
	5th	7	127	
	6th	5	132	
	7th	3	135	
	8th	3	138	
	9th	2	140	
	10th	1	141	
Hydrochloric acid	The mixture remained liquid after 2 hours and attained to its first hardening only after 12 hours. The second hardening occurred after 22 hours. It was still paste after 36 hours, and even after 68 hours when stirred, but at this time it had become somewhat crumbly.			
Nitric acid	Mixture acted in a similar fashion.			

To note the effect (Table V) of some organic liquids, two drops were mixed into a litharge-glycerine batch.

The characteristics of the reference mixture had changed in an inexplicable fashion, but, it does seem that all but benzene have the effect of increasing the time of hardening. One should hesitate to ascribe the difference between benzene and xylene, to the structural differences until further work is done.

During the previous summer with the assistance of Mr. Jarres we had tried the effect of various other organic materials, the results of which are recapitulated in Table VI.

Although this is to be considered a very preliminary survey and no serious quantitative observations have been made, the conclusion may be drawn that various substances do affect in various ways the rate of thixotropic changes. Hexamethylene tetramine appears to delay, while ethylamine aniline and mercapto benzothiazol appears to accelerate. Others have been found to ac-

TABLE III.

Material	Hardening	Time between hardenings	Time since mixing	Durometer reading
$Ba(OH)_2$	1st	29	29	
	2nd	27	56	
	3rd	19	75	
	4th	8	83	
	5th	10	93	
	6th	7	100	
	7th	5	105	
KOH	1st	27	27	
	2nd	21	48	
	3rd	11	59	
	4th	9	68	
	5th	6	74	
	6th	3	77	
	7th	3	80	
$Fe_2(OH)_3$	1st	72	72	15
	2nd	32	104	36
	3rd	17	121	56
	4th	9	130	85
	5th	6	136	100
	6th	5	141	
	7th	3	144	
	8th		147	
	9th		149	
	10th		151	
	11th		153	
	12th		155	
NaOH	1st	12	12	
	2nd	11	23	
	3rd	7	30	
	4th	3	33	
	5th	2	35	
NH_4OH	1st	17	17	5 drops of about 20 percent ammonia solutions were stirred into mix.
	2nd	14	31	
	3rd	9	40	
	4th	7	47	
	5th	5	52	
	6th	4	56	
	7th	5	61	

TABLE IV.

Hardening	Time between hardenings	Time since mixing	Hardening	Time between hardenings	Time since mixing
1st	23	23	5th	7	62
2nd	16	39	6th	5	67
3rd	8	47	7th	2	69
4th	8	55			

celerate, at least so far as these preliminary trials go, such as piperidine piperidyl dithiocarbamate, diphenyl biguanidine, tetramethylthiuram monosulfide, zimate, zinc butyl xanthate, phenyltolyl guanidine, and small amounts of water. Others that appear to delay are zinc isopropyl xanthate, potassium glycerol phosphate, potassium phenyl sulfate, aniline di-isopropyl thiophosphate and aldehyde ammonia and large amounts of water.

TABLE V. *Effect of organic liquids.*

Material	Hardening	Time between hardenings	Time since mixing
Litharge-glycerine alone	1st	87	87
	2nd	35	122
	3rd	19	141
	4th	13	154
Benzene	1st	87	87
	2nd	40	127
	3rd	18	145
	4th	13	158
	5th	11	168
	6th	8	177
	7th	7	184
Pyridene	1st	95	95
	2nd	41	136
	3rd	24	160
	4th	12	172
Aniline	1st	108	108
	2nd	43	151
Xylene	1st	109	109
	2nd	46	154
Phenyl hydrazine	1st	177	177
Paraldehyde (4 drops)	1st	113	113
	2nd	49	162

TABLE VI.

Substance	Effect	Color Change	Addenda
Triphenyl guanidine	None		Becomes very hard
Ethylidene aniline	Accelerated		
Zinc isopropyl xanthate	Delayed	Darker orange	After 14 hrs.—not hard
Piperidine piperidyl dithiocarbamate	Accelerated		
Hexa hexa	Delayed		
Phenyltolyl guanidine	None		Drier
Mercapto benzo thiazole	1st accelerated		Dry and crumby at 1st;
	2nd delayed		2nd quite fluid.
K-glycerol phosphate	Delayed		After 14 hrs.—not hard
A-16	Delayed?		After 14 hrs.—not hard
A-20	Delayed?		
K-ethyl xanthate	1st delayed	Brown, then	
	2nd accelerated	black.	
K-phenyl-sulphate	Delayed		
Diphenyl biguanidine	Accelerated	Light tan	
Tetramethylthiuram monosulfide	Accelerated	Dark tan	
Thio-anilide	None	Tan	
Zinc isopropyl xanthate	Accelerated		
Aniline di-isopropyl thiophosphate	Delayed		
Diphenyl guanidine	None		
Zn butyl xanthate	Accelerated	Dark brown	
Phenyltolyl guanidine	Accelerated		
Aldehyde ammonia	Delayed		
Tetramethyl thiuram disulfide	Slightly delayed		

VII. Variation in Samples of Litharge and Glycerine

The change in the characteristics of the simple litharge-glycerine mixture led us to inspect again the constancy of materials that were purchased from time to time. A series of observations along this line are shown in Table VII.

Table VII.

Sample	Hardening	Time between hardenings	Time since mixing	Durometer reading
I.	1st	27	27	
	2nd	32	59	
	3rd	20	79	
	4th	13	92	
	5th	9	101	
	6th		132	90
II	1st	25	25	
	2nd	31	56	
	3rd	20	76	
	4th	13	89	
	5th	8	97	
	6th	8	105	
	7th		130	90
III	1st	24	24	
	2nd	28	52	
	3rd	21	73	
	4th	12	85	
	5th	8	93	
	6th	7	100	
	7th		114	90
IV	1st	26	26	
	2nd	31	57	
	3rd	18	75	
	4th	12	87	
	5th	9	96	
	6th	9	105	
	7th		126	90
V	1st	26	26	
	2nd	29	55	
	3rd	18	73	
	4th	14	87	
	5th	13	100	
	6th		118	90

This table does not show on this day such extreme variations as we had found in the past. However, on the following day, the time for the first hardening had increased to 77 minutes for these samples.

It was suspected that the water in the glycerine was largely responsible for the wide and spurious variations. Some experiments were performed with glycerine which had been treated in various ways to remove water. Undried litharge was used in all cases. First ordinary undried glycerine was used; second, glycerine which had been heated four hours and had been kept in a glass stoppered bottle four days; third, glycerine which had been heated 7.5 hours at 110° on the same day that it was used; fourth, glycerine, which had been heated 8 hours and used the same day; fifth, glycerine which had been heated 8 hours the day before and kept in glass stoppered bottle; sixth, gly-

cerine which had been heated 4 hours, and placed in the calcium chloride desiccator under a vacuum; seventh, glycerine which had been heated 24 hours, kept in calcium chloride desiccator under vacuum, but which was drawn from a new supply. This glycerine was used with the three grades of litharge that were then on hand (*A*, *B*, *C*). The effects with the three different commercial grades of litharge differed widely, but showed variations that were consistent with the fact that the changes must have been due to a variation in some factor common to all the litharges. Such a factor may be water in the glycerine, or water in the atmosphere which was taken up during the time of mixing and of observing the samples.

In further experiments, we attempted to see just what effect the water in the litharge and glycerine as received may have. The general results expressed in terms of rate of hardening; that is, in the change of hardness in durometer scale units per minute, are as follows: When both glycerine and litharge were undried, the rate of hardening was 15.8; when the litharge only was dried by heating on a steam bath under a vacuum at 105°, the average rate of hardening was 11.2; when the glycerine only was dried, the average rate was 3.5; and when both glycerine and litharge were dried, the average rate of hardening became 2.5. The glycerine absorbs appreciably more water than the litharge, and the removal of the water from it to some extent will have a greater effect on the hardening rate.

It appeared from these observations on the drying of the glycerine that glycerine kept even in glass stoppered bottles for a few days became contaminated, or it may have been that the water absorbed by the glycerine during the mixing was sufficient to cause these variations. The relative humidity was not recorded while making these observations. It is quite clear, however, that the whole of the operation should be performed in a dry atmosphere. To get a further idea regarding the effect of water, a drying agent was added to the glycerine itself. Copper sulphate which had been entirely dried was accordingly dropped into the glycerine in fairly large amounts. There was always a discoloration of the solution in the neighborhood of the copper sulphate which one ordinarily would take as indicative of water. The glycerine itself had been dried and kept in a desiccator. The litharge-glycerine without the drying agent hardened to a durometer reading of 100 in 18 minutes, or at the rate of 5.6. When the glycerine is used which had in it copper sulphate and the copper sulphate was not filtered out of it, the average rate was 1.4; when this glycerine with the copper sulphate was filtered the rate became 1.7. When undried $CuSO_4$ was put into the glycerine, the rate was 1.6, which upon repeating became 2.0. Finally, a check with the original glycerine without the $CuSO_4$, the rate was 5.9, which compares very favorably with the initial rate observed at the beginning of this series, 5.6. Here again, the variations point in the direction in which the increase in water content might be expected to lead it. When the glycerine was filtered from the suspended $CuSO_4$ it was done under a desiccator so that the difference between the unfiltered and the filtered cannot be ascribed to the absorption of water vapor during the filtering, but must perhaps be ascribed to the water vapor which is absorbed during the few minutes of mixing, and

possibly during the subsequent time when the hardening process is under way. If it were chiefly the latter, however, one would expect to obtain a hard film since the water vapor should have to diffuse into the interior. Great differences in the hardness of the interior and of the surface is rather infrequent, but it has been observed on several occasions. Reference might be made here, too, to the marked case of a scab-like superficial layer when oleic acid was used in the mixture.

Several additional series of observations were made with glycerine which had been distilled under vacuum and the second third of the original sample which distilled over was used. In Table VIII are the effects of water on glycerine which had been so distilled and which came over uniformly at 194°F.

TABLE VIII.

Glycerine without water added			1 cc H_2O added			2 cc H_2O added		
Durometer	Time	Rate of hardening	Durometer	Time	Rate of hardening	Durometer	Time	Rate of hardening
7	19	0.37	9	14	0.64	9	9	1.0
21	25	0.84	27	21	1.28	55	16	3.4
50	32	1.56	75	27	2.78	100	22	4.6
70	36	1.94	90	30	3.00			
80	39	2.05	100	32	3.13			
95	42	2.26						

Water markedly increases the rate of hardening.

Neville[5] has observed this accelerating effect of water and acids on the rate of setting of litharge-glycerine cements.

In another paper a theory of the thixotropic transformation is given, together with a general discussion on the implication of the term and the occurrence of the phenomenon.

This work was carried out in the H. K. Cushing Laboratory of Experimental Medicine during the directorship of Dr. G. M. Stewart and Dr. J. M. Rogoff, whose generosity and encouragement we wish to acknowledge.

[5] Neville, Jour. Phys. Chem. **30**, 1181 (1926).

THE THERMO-STROMUHR METHOD OF MEASURING BLOOD FLOW*

By J. F. Herrick, Ph.D. and Edward J. Baldes, Ph.D.

Division of Physics and Biophysical Research

The Mayo Foundation, Rochester, Minnesota

(Received October 14, 1931)

Abstract

The purpose of the following article is to bring to the attention of the physicist, who is interested in the application of physics to physiology, a typical problem in biophysics. Rein, a physicist at the University of Freiburg, was confronted with the necessity of knowing accurately the blood supply to a certain organ. Because the various standard methods proved inadequate he developed an ingenious method which he calls the thermo-stromuhr. This method of determining blood flow has been modified in two respects: in the method of measuring the heating energy applied to the blood vessel, and in the method of construction of the diathermy-thermoelements. A tuned circuit is used which permits the measurement of resistance by the method of substitution. The diathermy-thermoelements are made from transparent bakelite and the process of construction is fully described. The theory of the thermo-stromuhr as well as the experimental application is explained in detail.

EVER since Harvey discovered the circulation of the blood in 1615 t e measurement of blood flow has been one of the fundamental problems confronting the physiologist. The importance of an accurate determination of the quantity of blood flowing in a blood vessel *in situ* needs no justification when we consider the many functions of the blood, of which the following are the most significant: (1) the transport of food and oxygen to every tissue of the body, (2) the removal of waste products, (3) the distribution of heat, and (4) the proper distribution of hormones (chemical substances made in one part of the body which are necessary for the normal regulation of other distant parts).

Certain physiologic processes reveal themselves only through a knowledge of blood flow. Many of these processes can never be completely understood by short-timed observations on the blood flow but only through continuous observations extending over hours and even days.

An ideal method for measuring blood flow would be one which permits continuous observations over long periods of time preserving most completely the normal physiologic conditions. Various standard methods for measuring blood flow have been developed and may be found in any standard textbook of physiology. However, none of these methods meets adequately the demands of the ideal method mentioned because: (1) they require the actual insertion,

* This paper is a section of a thesis submitted by J. F. Herrick to the Faculty of the Graduate School of the University of Minnesota in partial fulfillment of the requirements for the degree of doctor of philosophy in Biophysics, July, 1931. The remaining section will be published in a journal of physiology.

into the blood stream, of a part of the apparatus; this act produces two deleterious effects: the cutting of the blood vessel and the temporary damming up of the blood; (2) they require the use of anticoagulants if observations are to be extended over a considerable length of time, and (3) they do not permit the maintenance of normal body temperature and, since the mechanism for maintaining normal body temperature operates through the blood supply, a disturbance of it means a variation from the normal bood flow.

It might interest the physicist who is not familiar with the standard methods of measuring blood flow to know that these methods make use of such fundamental principles as those of the hydrometric pendulum, the Pitot's tube, the Venturi meter and radiation of heat.

Rein[1] has developed an ingenious method for the continuous measurement of the average absolute quantity of flow in closed blood vessels *in situ*. He has named his method the thermo-stromuhr. This method preserves most completely the normal physiologic conditions and allows simultaneous observations on several blood vessels. The latter possibility permits a study of certain regulatory mechanisms which operate through the blood. We have modified this method slightly and have applied it successfully to certain measurements of blood flow. The method is fundamentally this: at a definite place a small quantity of heat, as constant as possible, is supplied to the blood flowing in the blood vessel under observation and the resulting change in temperature is noted. It is obvious that the temperature change will be greater the more slowly the blood flows. The source of heat is a high-frequency alternating current (a clinical diathermy machine) of about 700 kilocycles. High-frequency alternating current is used because it does not produce unphysiologic conditions. Its only effect is that of heating. The temperature change in the blood is indicated by means of a sensitive differential thermocouple. The platinum electrodes from the high-frequency circuit, which are applied to the wall of the blood vessel, and the differential thermocouple are arranged in a single compendious unit called the diathermy-thermoelement (DThE). A detailed description of the construction of the DThE will be given later.

Since we detect the increase in the temperature of the blood by means of a differential thermocouple applied to the outside of the wall of the blood vessel, we are confronted with the problem of heat transfer from the flowing blood column across the wall to the measuring junctions. From fundamental considerations of heat transfer it is recognized that the quantity of heat, Q, exchanged between a fluid and its boundary wall is proportional to: (a) the heat-absorbing or heat-emitting surface, F, (b) the difference between the temperature of the fluid θ_F, and the temperature of the wall, θ_W, or $(\theta_F - \theta_W)$ and (c) the time during which the heat exchange takes place, t. To express this symbolically:

$$Q = \alpha \cdot F \cdot (\theta_F - \theta_W) \cdot t. \tag{1}$$

The proportionality factor α is known as the Wärmeübergangszahl (heat-transfer coefficient). There are various factors which influence the value of α

[1] Rein, Zeits. f. Biologie **87**, 394–418 (1928).

such as: the physiologic nature of the fluid; the velocity of flow; the nature of the heating and cooling surfaces especially with regard to roughness and homogeneity; the absolute temperature at which the process takes place; the various conceptions concerning the idea of average fluid temperature and the streaming flow.

The equation for the calculation of α in a straight tube of circular cross-section when applied to the fluid in the tube is (according to Gröber),[2]

$$\alpha \cdot \frac{d}{\lambda} = \psi\left(\frac{\omega \cdot d \cdot \rho}{\mu}, \frac{\omega \cdot d}{a}, \frac{z}{d}, \frac{\delta}{d}\right) \tag{2}$$

where d is the diameter of the tube, z the distance of the investigated cross-section from origin, δ the absolute roughness of the wall, ω the average streaming velocity, ρ the mass-density of the fluid, $[m \cdot t^2/l^4]$, μ the viscosity of the fluid, a the Temperature leitzahl $=\lambda/c \cdot \gamma$, where γ is the specific weight and c the specific heat and λ is the thermal conductivity. Most investigations refer to smooth tubes so that $\delta = 0$. In turbulent streaming, such as occurs in blood flow, the function ψ depends on the argument $\omega \cdot d \cdot \rho/\mu$ only in a very limited degree. For technical problems this argument may be disregarded. The above equation then becomes:

$$\alpha \cdot \frac{d}{\lambda} = \psi\left(\frac{\omega \cdot d}{a}, \frac{z}{d}\right). \tag{3}$$

According to Nusselt the general form of the function ψ is:

$$\alpha \frac{d}{\lambda} = K_1\left(\frac{z}{d}\right)^{K_2}\left(\frac{\omega \cdot d}{a}\right)^{K_3}. \tag{4}$$

Soennecken investigated the Wärmeübergangszahl for water flowing through metal tubes and arrived at the following equations: (a) a seamless drawn brass tube 17 mm inner diameter and 192 cm long:

$$\alpha = 2120(1 + 0.014 t_W)\frac{\omega^{0.91}}{d^{0.90}}$$

(b) Mannesmann precision steel tubes 192 cm long and diameters 17 mm and 28 mm:

$$\alpha = 735(1 + 0.014 \cdot t_W)\frac{\omega^{0.7}}{d^{0.3}}.$$

He stated that the differences between these two equations is due to the difference in roughness of the two tubes and not to the different metals *per se*.

Soennecken has shown that α depends on the inner wall temperature, while the influence of the average water temperature is to be disregarded.

Stender arrived at the opposite conclusion. He introduces a temperature τ in his calculations, which is defined by the following equation:

[2] Gröber, Wärmeübertragung, 1926.

$$\tau = 0.9t_m + 0.1t_W$$

where t_m is the average temperature of water in the entire tube and t_W is the average temperature of the tube wall. Thus α is determined almost alone by means of the average water temperature. He found the following equation to hold for steel and brass tubes of 17 and 28 mm diameter:

$$\alpha = 2830(1 + 0.0215\tau - 0.00007\tau^2)\omega^{0.091-0.00115\tau}.$$

According to Stender the dependency of α on the diameter of the tube is too insignificant to be indisputably established. For a more complete understanding of these equations the reader is referred to Gröber.

Generally one might write for water:

$$\alpha = K_\alpha \frac{\omega^{k_1}}{d^{k_2}}. \tag{5}$$

k_1 and k_2 in this equation are quite independent of those in the Nusselt equation. If V stands for the quantity of fluid passing by the place of observation in a unit of time with velocity ω, one may write:

$$V = \omega\pi r^2 = \omega\pi \cdot \frac{D_i^2}{4}$$

or

$$\omega = \frac{4V}{\pi D_i^2}.$$

Substituting the value of ω in the above expression for α:

$$\alpha = K_\alpha \cdot \frac{(4V)^{k_1}}{\pi^{k_1} \cdot D_i^{2+k_1+k_2}}. \tag{6}$$

$$k_1 > k_2;\ k_1 < 1.$$

According to the fundamental laws of heat conduction across a lamina:

$$Q = \lambda F \frac{\theta_2 - \theta_1}{\Delta} \tag{7}$$

where λ is the thermal conductivity, Q the quantity of heat conducted per second, $\theta_2 - \theta_1$ is the temperature difference, Δ is the thickness of lamina and F is the area of the lamina. Another way of writing the above equation is:

$$Q = -\lambda F \frac{d\theta}{dx}. \tag{8}$$

In applying the equation to the wall of the blood vessel where F is a variable because the different layers have different areas and where

$$F_i < F_a,$$

$$L\pi D_i < L\pi D_a.$$

F_i is the inner surface, F_a the outer surface, D_i the inner diameter, D_a the outer diameter, it is assumed that the quantity of heat flowing is the same in every layer. This means that the temperature gradient is continuously steeper because of the decreasing surface to be permeated. To express this symbolically

$$Q = -\lambda D\pi L \cdot 2\frac{d\theta}{dD}, \tag{9}$$

where L is the length of the observed portion of the tube, D the diameter of the tube, and θ the temperature.

Putting the above equation in a form for integration

$$\frac{dD}{D} = -2\pi\lambda\frac{L}{Q}d\theta$$

$$\int_{D_i}^{D_a}\frac{dD}{D} = \log D_a - \log D_i$$

$$\int_{\theta_{W_i}}^{\theta_{W_a}} d\theta = \theta_{W_a} - \theta_{W_i}.$$

Therefore

$$\log D_a - \log D_i = -2\pi\lambda\frac{L}{Q}(\theta_{W_a} - \theta_{W_i})$$

so that

$$Q = 2\pi\lambda L\frac{\theta_{W_i} - \theta_{W_a}}{\log (D_a/D_i)}. \tag{10}$$

Applying Eq. (1) to the problem at hand, $(t=1)$

$$Q = \alpha\cdot(\theta_B - \theta_{W_i})LD_i\cdot\pi. \tag{11}$$

From Eqs. (10) and (11) we have

$$\theta_{W_i} - \theta_{W_a} = \frac{Q\log (D_a/D_i)}{2\pi\lambda L}$$

$$\theta_B - \theta_{W_i} = \frac{Q}{\alpha L D_i\pi}.$$

Adding these equations

$$\theta_B - \theta_{W_a} = \frac{Q}{L\pi}\cdot\left[\frac{1}{\alpha D_i} + \frac{\log (D_a/D_i)}{2\lambda}\right] \text{ or}$$

$$\theta_{W_a} = \theta_B - \frac{Q}{L\pi}\left[\frac{1}{\alpha D_i} + \frac{\log (D_a/D_i)}{2\lambda}\right]. \tag{12}$$

If the electrical energy is completely absorbed, without loss, by the blood column moving homogeneously between the electrodes, and if the vessel walls can be neglected, the average temperature of the blood column, θ_B, is:

$$\theta_B = \frac{I^2R}{V} \text{ constant} \tag{13}$$

where R is the effective resistance, I the effective heating current, V the quantity of blood passing by the given point in unit of time. Assuming that the high-frequency current, which is the source of heating, warms only the blood passing between the electrodes, the vessel walls may be neglected when considering the mass to be warmed. Through experiment Rein found that the blood temperature was practically homogeneous under most variable stream conditions at a distance of at least $1.2 \times D$ (D = vessel diameter) from the heating electrodes. He also stated that heat equilibrium is well established and heat loss negligible at a distance of $1.2 \times D$ from the heating electrodes so that the Eq. (13) is sufficiently approximate.

Substituting this value of θ_B in Eq. (12):

$$\theta_{W_a} = K\frac{I^2R}{V} - \frac{Q}{L\pi}\cdot\left[\frac{1}{\alpha D_i} + \frac{\log (D_a/D_i)}{2\lambda}\right].$$

Substituting the value for α as given in Eq. (6):

$$\theta_{W_a} = K\frac{I^2R}{V} - \frac{Q}{L\pi}\left[\frac{D_i^{1+k_1+k_2}\cdot\pi^{k_1}}{K_a\cdot(4V)^{k_1}} + \frac{\log (D_a/D_i)}{2\lambda}\right] \tag{14}$$

From Eq. (14) we see that the temperature of the wall of the blood vessel which we are considering depends on two factors: (1) inversely on V, the quantity of fluid passing the point of observation in a unit of time, and (2) directly on the heat developed in the vessel, that is, I^2R. If there is heat flow toward the outside, this must be corrected according to the second term of the equation. Thus, there appear two special cases.

Case 1.—Where Q is negligible, and the equation becomes:

$$\theta_{W_a} = K\frac{I^2R}{V}.$$

This equation indicates that the relation between the blood flow, V, and the vessel wall temperature, θ_{W_a}, may be represented as an equilateral hyperbola with coordinates as asymptotes.

Case 2.—Where Q may not be considered as negligible; this is largely dependent on the proper application of the measuring thermoelements. In this case the relation between blood flow and the vessel wall temperature deviates from the equilateral hyperbola. The wall temperature for one and the same blood vessel depends on a negative power of V. The exponent is always smaller than 1.

The fundamental theory of the thermo-stromuhr is not satisfactory for the present because the two important factors, that is, the Wärmeübergang-

szahl (α) and the Warmeleitzahl (λ) for the vessel wall are unknown. Also the α and λ for the blood may not be regarded as similar to the α and λ for water. The reliability of the thermo-stromuhr as a method for measuring blood flow has been shown experimentally by the fact that there exists a definite relation between the average blood flow and the temperature of the wall of the blood vessel. The success of the method depends largely on the production and measurement of the heating energy continuously applied to the blood in the vessel.

Figure 1 shows a diagram of the circuit employed. As stated, a clinical diathermy machine (Victor Vario-Frequency Diathermy apparatus) is the source of high-frequency current. The frequency employed is about 700 kilo-

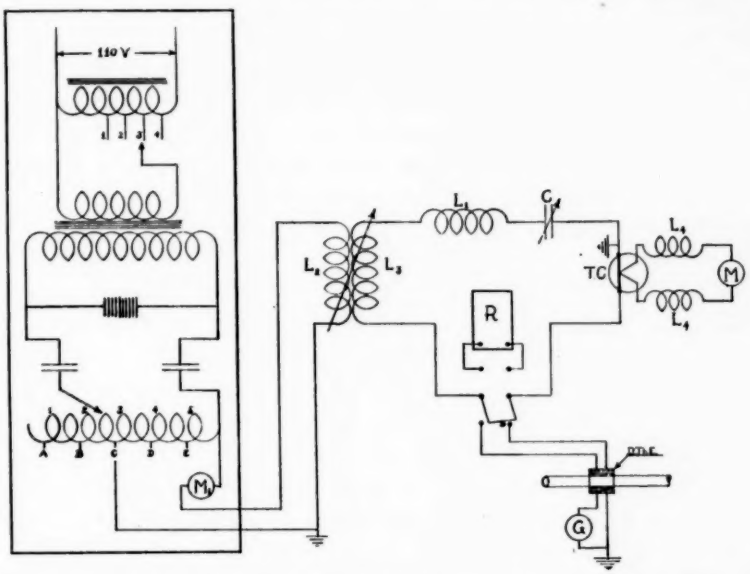

Fig. 1. Diagram of high-frequency circuit. *TC*, vacuum thermocouple. *M*, microammeter. *R*, resistance box. *G*, Zeiss loop galvanometer. *DThE*, diathermy-thermoelement. L_1, L_2, L_3, inductance coils. L_4, high frequency choke coils.

Heavy black line incloses clinical diathermy machine circuit.

cycles. This particular circuit is marked off by a heavy black line. The remainder of the high-frequency circuit constitutes the measuring arrangement. This circuit permits careful tuning by means of a variable condenser. A tuned circuit allows the resistance of the blood vessel with its flowing blood to be measured by the method of substitution. A resistance box made by the General Radio Company is used in which the capacity and inductance effects are negligible. The current is measured by means of a vacuum thermocouple. The particular thermocouple employed has the following specifications: normal current, 50 m.a.; maximum current, 85 m.a.; heater resistance, 13 ohms; couple resistance, 12 ohms. A microammeter of 39.3 ohms resistance is connected through choke coils to the couple circuit. This microammeter together with the choke coils and thermocouple was carefully calibrated with low frequency alternating current. The circuit is grounded as indicated in the dia-

gram so that any capacities introduced, such as when the animal is put in circuit, are negligible in comparison to the earth's capacity.

Having measured the resistance of the blood vessel containing its flowing blood and also the current passing through it, the total energy input in terms of calories per second may be calculated according to the formula $0.24I^2R = H$.

The difference in temperature between two points on the outside of the wall of the blood vessel at equal distances (at least 1.2 × the diameter of the blood vessel) upstream and downstream from the heating electrodes is observed. This is accomplished by connecting a differential thermocouple to a Zeiss loop galvanometer, the sensitivity of which is 6×10^{-8} amperes for the position in which it is used.

Very fundamental to the success of the thermo-stromuhr method of measuring blood flow is the correct construction of the diathermy-thermoelements and for this reason a rather detailed description of the construction will be given. Figure 2 is a mechanical drawing illustrating the method of construction. The size of the blood vessel most commonly used has been about 3 mm and this necessitates an insulation block about 9 mm square and 13 mm long in which a groove, somewhat less than the size of the blood vessel, has been milled to a depth of about 4 mm.

The insulation block of transparent bakelite is prepared as follows. The two slots *ee'* and *ff'* are made in the bottom by using first a coarse saw and then a fine saw. These definitely determine the exact position of the small glass tubes in which the thermocouples are placed. Next the slot *cc'* is made midway between *ee'* and *ff'* to allow proper installation of the diathermy plates. After the fine slot *aa'* has been made to imbed the constantan wire, the block is ready for the drilling of the holes 1, 2, 3, 4, which are of two sizes as illustrated, the upper portion of the hole being large enough to receive the rubber tubing used for insulation while the smaller hole allows the passage of the lead wire only.

The thermocouples are made of copper constantan wires each of 0.05 mm diameter. The constantan wire is insulated from the high-frequency current by glass tubing in addition to the resin insulation. The thermojunctions are placed in thin-walled glass tubes about 5 mm long and with a bore slightly larger than twice the diameter of the thermocouple wire. The length of the constantan wire is chosen so that when placed in the slit *aa'* the ends will form the junctions with the copper wire at *x* and *x'*. The thermocouple unit is then set in place and anchored with molten resin. Manipulation of the resin is facilitated by the use of an electrically heated loop of resistance wire. The flexible lead wires (habitual) are now soldered and brought out through holes 1 and 4.

The diathermy electrodes are thin platinum plates, about 2 × 3 mm, to the center of which is soldered a small copper wire. The plates are held in place by resin and the small copper wire is led through the appropriate slot and then soldered to the flexible lead wires which are brought out through holes 2 and 3.

After several series of experiments Rein found that the relation between

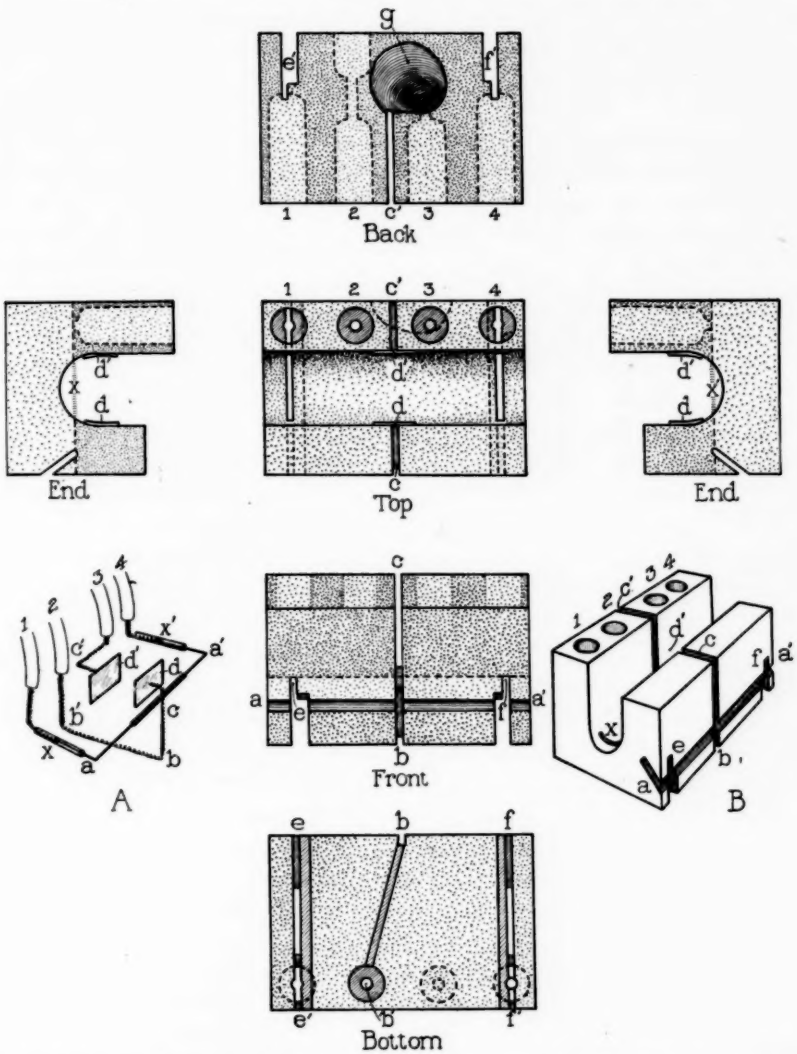

Fig. 2. Mechanical drawing of diathermy-thermoelement. Insert *A* illustrates the wiring only. The constantan wire is represented by straight lines and the copper by coiled. Each section of the wiring is lettered in accordance with the slot in which it lies. Insert *B* is a perspective of the insulation block preparatory to the installation of the thermocouples and diathermy plates.

The section of constantan wire *aa'* in insert *A* is placed in slot *aa'* shown in front view and insert *B*. It may be noted that it is threaded through glass capillary tubing for insulating purposes. From *a* and *a'* the constantan wire goes to points *x* and *x'* through the slots *e* and *f* (front and bottom views). At the points *x* and *x'* the constantan is soldered to copper wires which are introduced through slots *e'* and *f'* (back and bottom views). A glass capillary tube is placed on the wire at this point for insulation. It bridges the arch shown at *x* and *x'* (end views). The copper wires are then soldered to lead wires inserted in holes 1 and 4 (top and back views).

The diathermy plates *d* and *d'* are placed as shown in top and end views. A copper wire is soldered to plate *d'*. This wire *c'* is brought through slot *c'* (top and back views) where it is soldered to a lead wire which has been introduced in hole 3. The opening *g* is made to facilitate this procedure.

A wire *c* (insert *A*) is soldered to plate *d* and brought through slot *c* to point *b* (top and front views). The section of wire *bb'* (insert *A*) is placed in slot *bb'* (bottom views). Here it is soldered to a lead wire which has been inserted in hole 2.

Rubber tubing is placed on all leads at holes 1–2–3–4 which are drilled large enough to accommodate it and made fast with flexible collodion.

the Zeiss loop galvanometer deflections (G) and the quantity of blood flowing through the examined vessel in a unit of time (V) was

$$GV^{\beta} = \text{const. } I^2R = K$$

for a constant energy input. The constants β and K are determined experimentally. They vary for each DThE and are known as the characteristics of the DThE. The experimental procedure for evaluating β and K is as follows: The DThE is carefully applied to a fresh living carotid of a dog. The excised carotid is placed in a constant humidity chamber kept at room temperature. Fresh defibrinated blood is conducted from a Mariotte bottle elevated to a height which produces a hydrostatic pressure equivalent to that of dog's blood pressure (120 mm Hg). After flowing through the model the blood is collected in a graduate tube and the time of flow carefully noted. The carotid, the DThE and the blood are kept at room temperature. The temperature of the blood is immaterial provided the DThE is kept at the same temperature. To insure an undisturbed position of the blood vessel in the DThE a drop of collodion is placed on the top of the blood vessel after placing it carefully in the DThE. The collodion congeals in an instant and holds the vessel firmly, without obstruction, in the groove of the DThE. The first thing to be measured is the resistance of the blood vessel through which the blood is flowing. The magnitude of this resistance determines the intensity of the heating current used because the blood is not heated more than 0.1°C. The energy input is kept constant throughout the experiment. After the deflection of the loop galvanometer is well established for a given rate of flow it is then observed using a different rate of flow. From these known values of G and V, the constants β and K may be computed. In addition to β and K, the exact value of the energy input during the experiment, J_e, must be recorded. The DThE is now ready to be applied to the blood vessel *in situ*.

The correct fit of the DThE is the most fundamental condition for the success of all measurements in the living animal. The correctness of fit is tested as follows: (1) the null position of the Zeiss loop galvanometer must not change on the introduction of the unheated thermojunctions. If it does shift with pulsating or respiratory fluctuations, the DThE is too wide and the blood vessel is lifting itself off from the junctions periodically. (2) Upon turning on the heating current, the Zeiss loop galvanometer deflects an amount depending on the rate of blood flow. After this deflection is well established, doubling the energy input should produce twice the deflection. (The wound is closed tightly after the introduction of the DThE so that the body temperature is maintained about the DThE.)

The foregoing controls should be repeated several times throughout any experiment. One should not proceed with the experiment if these controls are unsatisfactory.

At this point the reader may be wondering how the calibration of the DThE with a steady flow can be used for estimating an intermittent flow in the blood vessel of the animal. It has been shown experimentally by Rein that the thermo-stromuhr responds to an intermittent flow merely by indicating the average flow of blood.

One scarcely ever uses the same energy input for both calibration and animal experiment because that energy input is used which gives a desirable sensitivity. The magnitude of K obtained in the calibration experiments changes linearly with the energy input:

$$\frac{K^1}{K} = \frac{J_v}{J_e} \text{ or } K^1 = \frac{KJ_v}{J_e}$$

where J_v is the energy input during the animal experiment and J_e is the energy input during the calibration experiment. For the animal experiment in which J_v differs from J_e:

$$GV^\beta = K'$$

$$GV^\beta = \frac{KJ_v}{J_e}$$

$$V = \left(\frac{KJ_v}{GJ_e}\right)^{1/\beta}.$$

Before applying the thermo-stromuhr in the investigations mentioned below the method was thoroughly checked and found to be reliable to about 10 percent. This experimental error is not considered unusual in biological measurements. The investigations carried on, thus far, with our modification of the thermo-stomuhr are: (1) the blood flow of the kidney during the intravenous injection of a diuretic and during the subsequent diuresis; (2) the effect of sectioning the renal nerves on the blood flow of the kidney; (3) the effect of the removal of one kidney on the blood flow of the other; (4) the blood flow of the transplanted kidney during the intravenous injection of certain diuretics and drugs, and (5) the blood flow of the femoral artery under various conditions. The results of these investigations will be published in a journal of physiology.

THE EDITOR'S COLUMN

The Production of High Velocity Charged Particles: An Addition

IN THE note under this title in these columns last month no mention was made of a very promising method for the production of high potentials which has been recently developed. The writer had overlooked the brief report of the experiment.[1] In idea the apparatus is very simple, and at first glance even seems almost naïve, but it illustrates the fact that even now important developments are still to be made by the intelligent application of simple principles. In its essentials the apparatus consists of a spherical shell in the center of which is fixed a pulley around which an endless silken belt travels, the belt passing out of the sphere through a hole without touching, and over a second pulley at some distance from the sphere. This second pulley is grounded while the pulley inside is in electrical contact with the sphere. As the belt leaves the grounded pulley travelling toward the sphere a brush discharge maintained by a kenetron set actuated from the light circuit plays on the belt so that the latter becomes charged with electricity which is carried along with it as a bound charge into the sphere. As the belt passes over the inside pulley its charge is removed, and by the well-known property of electricity to collect on the outside of a closed conducting surface, the charge passes to the outside of the sphere which then becomes charged. The process is continuous as the endless belt keeps travelling around, so that ultimately the sphere will be charged up to a very high potential. Two identical units developing opposite potentials are used. With rather small spheres (24 inches in diameter) potential differences of around one and one half million volts have been obtained, the potential obtained being limited by the discharge from the sphere. Plans are afoot for the construction of an apparatus with spheres of some 15 feet in diameter, with which much higher voltages can be obtained.

[1] R. J. Van DeGraff, Phys. Rev. **38,** 1919 (1931). Program of the Schenectady meeting.

The Indetermination Principle in Quantum Mechanics

TO THE mind of the physicist trained in the rigors of the classical or Newtonian mechanics, one of the most puzzling features of the new mechanics is that it gives one no way of following in time the exact motion of a particle, say of an electron. The end and ultimate aim of the solution of a problem by Newton's methods is to find a formula for the coördinates of the particle as functions of the time t. When the forces acting on the particle are known, and when the initial position and the initial velocity of the particle are specified, then one finds, on solving the equations of motion, the equation for the path followed by the particle. Of course in many cases one may not be able to actually solve these equations of motion, but from a general point of view this difficulty is of secondary importance since one has no particular reason to doubt the existence of such a solution which he might find if he were sufficiently clever.

In the wave mechanics, on the other hand, when one has solved a problem he does not obtain equations for the coordinates as functions of the time, but instead obtains only a certain function Ψ which is a function of the coordinates x, y, z, as well as t; all four of these quantities thus appear as independent variables, Ψ itself being the dependent variable. This function Ψ is interpreted by making the hypothesis that the probability of finding the particle in the little volume $dxdydz$ having its mid-point at the point x, y, z, at the instant t, is $|\Psi(x, y, z, t)|^2$. Generally speaking, $\Psi(x, y, z, t)$ is a complex number and $|\Psi(x, y, z, t)|^2$ means the square of the magnitude (modulus) of Ψ. Since Ψ is obtained by solving a partial differential equation which is in many ways similar to the equation which governs light waves or radio waves, it is sometimes called the "wave function". This also is the excuse for speaking of a "wave mechanics".

It would perhaps be better if scientists would agree to drop this designation and would speak rather of the "quantum mechanics".

It is perhaps hard for physicists to whom the Newtonian system of dynamics has been the corner-stone and pillar of science to believe that there is any stuff and substance in this procedure of quantum mechanics. Many are undoubtedly wont to feel that we have taken a step backward in giving up the clear and exact picture of motion which was paramount in the classical method, and in substituting for it only an idea of probability. Of course, the first and indisputable excuse for any theory comes from its success in predicting the facts which we observe in Nature, and of such success on the part of the quantum mechanics there is no question. But one cannot be satisfied with even a successful theory if he feels that he does not understand it. In such a predicament one can follow one of two courses: he can abandon the theory in spite of its successes and try to build up another which will also explain the facts but which will make the phenomena more easily understandable to him, or he can assume the correctness of the theory and then attempt to build up a set of mental pictures which will allow him to interpret the theory to his own satisfaction. Either procedure is, of course, in perfect accordance with the basic aims of science, and that course is to be chosen which seems to offer the best means of making progress, although one's inclination impels him to try first to understand that theory which is already known to give an explanation of the phenomena.

THIS is exactly the situation which arose in the field of atomic physics about 1926. The initial conquests of the matrix theory of Heisenberg and Born, the q-number theory of Dirac, and the wave mechanics of de Broglie and Schrödinger were so startling as to leave small doubt that they represented an advance of a fundamental nature. This feeling was immeasurably strengthened when it was discovered that these apparently diverse theories were in reality but different mathematical aspects of one general theory. What then was one to do about it? The evidence was so strong that there was but one course for physicists to follow: it was imperative that one should try to find a set of mental pictures of the behaviour of electrons and protons which would fit into the mathematical theory and yet which would give one a certain intuitive understanding of the situation. Apart from those developments which have dealt with the application of the mathematical theory to specific problems the history of the quantum mechanics since its inception has been largely the history of the attempts of the theoretical physicist to adjust his mental pictures. Contrary to popular belief, not even a "quantum physicist" can work without mental images.

Heisenberg[1] attacked the problem first of explaining why one does not need to vizualize the motion of an electron as completely as is done in the classical mechanics; i.e., why it is not necessary to have formulas for the coördinates of the electron expressed as functions of the time t. He argued that a theory should yield no more results than can be obtained by making experimental observations on the system (i.e., the electron). Now if one makes an observation on an electron in an atom or on a free electron in a discharge tube, one must cause it to be acted upon in some way, say by a beam of light which it scatters. But in the act of scattering the light the electron will suffer a deviation so that it will no longer travel along its original path with its original velocity; the process of making a measurement on the electron has disturbed it. This is in itself not really a new idea since anyone who makes measurements of any sort realizes perfectly well that he disturbs the apparatus in the process. Heisenberg's particular point lay in making it clear that in atomic processes the magnitude of the disturbance is roughly as large as the energy of the system itself, and that more serious still, the exact effect produced by the disturbance cannot be predicted beforehand so that the motion of the particle after the disturbance has ceased is somewhat uncertain. It would thus not be possible to make successive observations on the same electron in order to determine the path which it would follow if it were not disturbed at all since the very first observation would completely upset the motion. Since it is impossible to actually observe the path followed by the particle, one can suppose that this is useless information with which one can readily dispense. On the other hand it is possible to argue that by making a series of observations on a

[1] See especially his book "The Physical Principles of the Quantum Theory," University of Chicago Press (1930).

number of identical systems, say on a number of hydrogen atoms, one might actually determine the probability of finding the electron at any given point within the atom, as so determine the modulus of Ψ directly. Since Ψ is a complex quantity there would still be a certain part of it which would not be observable in this way, but in any event there would be a close connection between $|\Psi|^2$ and the experimentally observable probability for locating the electron at a given point.

Following along on this tack Heisenberg discussed experiments by means of which one might attempt to measure the velocity of an electron. Here he uncovered an analogous difficulty: in order to measure the position of an electron one is obliged to produce an indeterminate change in its momentum, and conversely in measuring the velocity or momentum of an electron, the disturbance caused by the experiment makes the path followed by the electron uncertain so that there is an indeterminacy in its position. This reciprocal indeterminacy in the disturbance of the velocity or position of an electron which would be produced by a measurement of the other quantity was elevated by Heisenberg to the dignity of a principle of Nature, and was crystallized by him in the mathematical form of his famous "uncertainty" or "indetermination" relations. According to these relations the uncertainties produced in either the velocity or position of the electron by a measurement of the other are related in such a way that if Δv_x and Δx are the corresponding uncertainties, then the product $(\Delta v_x)(\Delta x)$ is of the order of magnitude of h/m where h is Planck's constant and m is the mass of the electron. The value h/m acts as the lower limit for the product $(\Delta v_x)(\Delta x)$.

Heisenberg's arguments are, as we see, based upon the consideration of the results to be obtained by actually performing experiments on the system; i.e., on the electron. It is thus necessary that one consider not only the system about which one desires some information, that is, the electron, hydrogen atom, etc., but also some "external agency" such as a beam of light by means of which one proposes to perform an experiment upon the electron or the hydrogen atom.

These uncertainty relations of Heisenberg can be obtained, however, in a quite different manner which makes no mention of an external perturbing system. One simply observes that since the electron is not localized at a fixed point, there is a probability that it will be found at points other than its mean position. One can then define the uncertainty in the coordinate x; i.e., Δx as the root mean square value of the deviation of x from its mean value.[2] This is just the same procedure as is followed in statistics when one calculates the standard deviation of a set of numbers from their mean. The set of numbers is here the values of x, each value being weighted by the probability that the electron will have that value for its x coordinate. In an analogous manner one can define the uncertainty in the velocity (or momentum) of the electron; in order to do this one must first define, as is done in quantum mechanics, the function which gives the probability that the velocity of the electron will have the value v_x. On calculating Δv_x and Δx in this manner it is found that they satisfy relations of just the sort discovered by Heisenberg.

THERE are thus two ways of viewing these "uncertainty" relations; two ways which seem logically distinct. The first makes fundamental the interaction of the system in question with some outside agency, while the other mentions only the properties of the system itself as calculated from the function Ψ. They are connected of course, through the assumption that if one were able to make an accurate experimental determination of the probability of finding the electron at a given point, or of its having a given velocity, then one would obtain the same result as he would by calculating this probability from the mathematical postulates of quantum mechanics. It may be noticed that in the sense of this second definition one could consider a Δx and Δv_x even if the electron obeyed the classical mechanics.[3]

Whether or not one can obtain any clearer general picture than this for the motion of an electron as specified by quantum mechanics is a question. Arguments have been proposed

---

[2] E. U. Condon, Science **69**, 573 (1929); H. P. Robertson, Phys. Rev. **34**, 163 (1929); H. Weyl, "Gruppentheorie und Quantenmechanik," p. 67; W. Heisenberg "The Physical Principles of Quantum Theory," p. 16. Heisenberg defines Δx as $2^{1/2}$ times the standard deviation of x.

[3] Cf. Heisenberg, reference 1, p. 30.

based upon the use of concentrated wave packets.[4] A wave packet is a region within which Ψ has a finite value while outside of this region Ψ has a negligible value. Such a concentrated wave packet can thus be used to describe the fact that the electron is certainly within this very small region of space. By following the motion of the packet as it is governed by Schrödinger's equation one obtains a semi-classical picture of the motion of the electron which is located within the packet. Unfortunately for descriptive purposes one finds that the wave packet expands as time goes on so that the region within which the electron is located becomes larger and larger, and one soon loses track of the electron.

[4] Cf. N. Bohr, Nature **121,** 580 (1928); C. G. Darwin, Proc. Roy. Soc. **A117,** 258 (1928); Annales de l'Institut Henri Poincaré **1,** 25.

E. L. HILL

ERRATA

AN ELECTROMAGNETICALLY CONTROLLED THREE-ELECTRODE VACUUM TUBE

By F. B. Haynes

Physics, September, 1931

Page 193, line 5, read "clockwise" for "counter clockwise".

Page 193, line 6, read "counter clockwise" for "clockwise".

AUTHOR INDEX TO VOLUME 1

References with (EC) are from the Editor's Column

Ambrose, H. A. and A. G. Loomis. Some colloidal properties of bentonite suspensions—129
Andrews, H. L. A New method of dielectric constant measurement at radio frequencies—366
Austin, J. B. Temperature distribution in solid bodies during heating or cooling—75

Baldes, Edward J. (see Herrick, J. F.)—407
Bleininger, A. V. Application of physics in ceramics—268
Botset, H. G. (see M. Muskat)—27
Busang, P. F. (see Smith, W. O.)—18
Buchta, J. W. X-ray wave-lengths, crystal structures and fundamental constants—137 (EC)

Cartwright, C. Hawley. Natural observation limit of radiometric measurements—211
Compton, Arthur H. Human value of physics—13
Coolidge, W. D., L. E. Dempster and H. E. Tanis, Jr. High voltage cathode ray and x-ray tubes and their operation—230

Dempster, L. E. (see Coolidge, W. D.)—230

Foote, Paul D. (see Smith, W. O.)—18
Foster, L. V. Limitations and adaptability of ultramicroscopes to the study of colloid systems—154
Fricke, Hugo. Electric conductivity and capacity of disperse systems—106

Gill, Stanley and W. F. Rogers. Relation of long line currents to soil corrosion—194
Gillett, H. W. and H. W. Russell. Comments on the application of physics to metallurgy—1

Hartig, H. E. Charts for transmission line problems —380
Haynes, F. B. Electromagnetically controlled three-electrode vacuum tube—192; erratum, 422
Herrick, J. F. and Edward J. Baldes. Thermostromuhr method of measuring blood flow—407
Hill, E. L. Hyperfine structure and the constitution of nuclei—139 (EC)
——— Indetermination principle in quantum mechanics—418 (EC)
——— Light quanta and electrodynamics—208 (EC)
——— Production of high velocity charged particles—341 (EC)
——— Production of high velocity charged particles: An addition—418 (EC)
——— Quantum theory of the metallic state—271 (EC)
——— Reflection of electrons in quantum mechanics— 206 (EC)
——— Spinor calculus—340 (EC)
——— System of "atomic" nuclei—205 (EC)
——— Theories of the electron—141 (EC)
——— Vectorial photoelectric effect—207 (EC)
Hooper, W. J. The deposition of dust on walls—61

Karrer, E. and P. Wasserman. Thixotropy of litharge and glycerine—393
Kennedy, R. G., Jr. (see Sager, T. P.)—352
Kingdon, K. H. and H. E. Thomson. Experiments with gas-filled Cs-O-Ag Photo cells—343

Langmuir, I. and W. F. Westendorp. Study of light signals in aviation and navigation—273
Loomis, A. G. (see Ambrose, H. A.)—129

McCollough, E. E. Thermal expansion of some aluminum alloys—334
McKeehan, L. W. Magnetic sharpener—388
Muskat, M. and H. G. Botset. Flow of gas through porous materials—27

Nelson, Herbert. Some thermionic properties of barium films adsorbed on tungsten—84
Nichols, J. B. Application of the ultracentrifuge to some colloid-physical problems—254

Rashevsky, N. Some theoretical aspects of the biological applications of physics of disperse systems—143
Reynolds, Neil B. Studies with an ionization gauge—182
Richards, L. A. Capillary conduction of liquids through porous mediums—318
Rogers, W. F. (see Gill, Stanley)—194
Russell, H. W. (see Gillett, H. W.)—1

Sager, T. P. and R. G. Kennedy, Jr. Use of glycolphthalic anhydride resin as a high-vacuum cement —352
Scott, Merit. Effect of the presence of a grid upon certain characteristics of the airflow at the surface of an airfoil—94
——— Experimental method of determining certain characteristics of the flow at the surface of an airfoil—48
Smith, W. O., Paul D. Foote, and P. F. Busang. Capillary rise in sands of uniform spherical grains —18

Stamm, Alfred J. Three methods of studying capillary structure as applied to wood—116
Steele, F. A. Physics in the study of pigment dispersions—101
Suits, Chauncey Guy. Voltage selective nonlinear bridge—171
Swartz, C. A. Variation in the surface tension of gas-saturated petroleum with pressure of saturation—245

Tanis, H. E., Jr. (see Coolidge, W. D.)—230
Thomsen, H. E. (see Kingdon, K. H.)—343
Tiedeman, John A. Time lag of the electric spark—354

Van Vleck, J. H. Valence forces in chemistry—69 (EC)
——— Equations of state of gases—71 (EC)
——— Classical approximations in quantum mechanics—72 (EC)
——— Photographic models of the charge distribution in atoms—73 (EC)
——— Transmission coefficients in thermionics—74 (EC)

Wasserman, P. (see Karrer, E.)—393
Welo, Lars A. Conductivities of low order in hydrocarbons and transformer oil—160
Westendorp, W. F. (see Langmuir, I.)—273

ANALYTIC SUBJECT INDEX TO VOLUME 1

Airfoils
Flow at the surface, Merit Scott—48, 94
Alloys
Aluminum, thermal expansion, E. E. McCollough —334
Aviation
Light signals for, I. Langmuir, W. F. Westerdorp —273

Biophysics
Biological applications of physics of disperse systems, N. Rashevsky—143
Measurement of blood flow, J. F. Herrick, Edward J. Baldes—407
Blood Flow
Thermo-stromuhr method of measuring, J. F. Herrick, Edward J. Baldes—407

Capillarity (see also Surface tension)
Conduction of liquids through porous mediums, theory and data on soils, L. A. Richards—318
In sands, W. O. Smith, Paul D. Foote, P. F. Busang—18
Structure of wood, Alfred J. Stamm—116
Surface tension of gas-saturated petroleum, C. A. Swartz—245
Cathode rays
High voltage cathode ray and x-ray tubes, W. D. Coolidge, L. E. Dempster, H. E. Tanis, Jr.—230
Cements
Glycol-phthalic anhydride resin as a high-vacuum cement, T. P. Sager and R. G. Kennedy, Jr.—352
Ceramics
Applications of physics, A. V. Bleininger—268
Colloids
Adaptability of ultramicroscopes to the study of colloid systems, L. V. Foster—154
Application of the ultracentrifuge, J. B. Nichols—254
Bentonite suspensions, H. A. Ambrose, A. G. Loomis—129
Electric conductivity and capacity of disperse systems, Hugo Fricke—106
Physics in the study of pigment dispersions, F. A. Steele—101
Contact potentials
Of barium films adsorbed on tungsten, Herbert Nelson—84
Corrosion of pipe lines
Long line currents, Stanley Gill, W. F. Rogers—194

Dielectric constant
Measurement at radio frequencies of N_2, H. L. Andrews—366
Disperse systems
Application of physics to, F. A. Steele—101
Biological applications of physics of, N. Rashevsky —143
Electric conductivity and capacity of, Hugo Fricke—106
Drilling fluids
Bentonite suspensions, H. A. Ambrose, A. G. Loomis—129
Dust
Deposition on walls, W. J. Hooper—61

Editor's Column
Classical approximations in quantum mechanics, J. H. Van Vleck—72
Equations of state of gases, J. H. Van Vleck—71
Hyperfine structure and the constitution of nuclei, E. L. Hill—139
Indetermination principle in quantum mechanics, E. L. Hill—418
Light quanta and electrodynamics, E. L. Hill—208
Photographic models of the charge distribution in atoms, J. H. Van Vleck—73
Production of high velocity charged particles, E. L. Hill—341
Production of high velocity charged particles: An addition, E. L. Hill—418
Quantum theory of the metallic state, E. L. Hill—271
Reflection of electrons in quantum mechanics, E. L. Hill—206
Spinor calculus, E. L. Hill—340
System of "atomic" nuclei, E. L. Hill—205
Theories of the electron, E. L. Hill—141
Transmission coefficients in thermionics, J. H. Van Vleck—74
Valence forces in chemistry, J. H. Van Vleck—69
Vectorial photoelectric effect, E. L. Hill—207
X-ray wave-lengths, crystal structures and fundamental constants, J. W. Buchta—137
Electrical conductivity
Of disperse systems, Hugo Fricke—106
Of hydrocarbons and transformer oil, Lars A. Welo—160

Electrical lines
Charts for *E*, *I*, and *Z* of long lines, H. E. Hartig—380
Electrical Discharge
Time lag of the electric spark, John A. Tiedeman—354
Errata
Electromagnetically controlled three-electrode vacuum tube, F. B. Haynes—422
Gases
Flow of heat at surface of airfoil, Merit Scott—48; effect of grid, Merit Scott—94
Flow through porous materials, gas wells, flow from, M. Muskat, H. G. Botset—27
Heat
Flow at surface of airfoil, Merit Scott—48, 94
Temperature distribution in solid bodies, J. B. Austin—75
Human value of physics
Arthur H. Compton—13
Instruments and methods
Adaptability of ultramicroscopes to the study of colloid systems, L. V. Foster—154
Application of the ultra entrifuge to colloid-physical problems, J. B. Nichols—254
Charts for transmission line problems, H. E. Hartig—380
Dielectric constant measurement at radio frequencies, H. L. Andrews—366
Electromagnetically controlled three-electrode vacuum tube, F. B. Haynes—192; erratum—422
Gas-filled Cs-O-Ag photo-cells, K. H. Kingdon and H. E. Thomson—343
Glycol-phthalic anhydride resin as a high-vacuum cement, T. P. Sager and R. G. Kennedy, Jr.—352
High voltage cathode ray and x-ray tubes, W. D. Coolidge, L. E. Dempster, H. E. Tanis, Jr.—230
Ionization gauge, studies, Neil B. Reynolds—182
Long line currents in buried pipes; measurements of, Stanley Gill, W. F. Rogers—194
Magnetic sharpener, L. W. McKeehan—388
Methods of studying capillary structure as applied to wood, Alfred J. Stamm—116
Radiometric measurements; observation limit of, C. Hawley Cartwright—211
Removing foreign material from hydrocarbons, Lars A. Welo—160
Selective differential photoelectric receiver, I. Langmuir, W. F. Westendorp—273
Thermo-stromuhr method of measuring blood flow, J. F. Herrick, Edward J. Baldes—407
Time lag of the electric spark, John A. Tiedeman—354
Voltage selective nonlinear bridge; selective relay, Chauncey Guy Suits—171
Kinetic theory (see **Gases**)
Lath marks
Deposition of dust on walls, W. J. Hooper—61
Light signals
In aviation and navigation, I. Langmuir, W. F. Westendorp—273
Liquids
Capillary conduction of water in soils, L. A. Richards—318
Capillary rise in sands, W. O. Smith, Paul D. Foote, P. F. Busang—18
Metallurgy
Applications of physics to, H. W. Gillett, H. W. Russell—1
Photoelectricity
Gas-filled Cs-O-Ag photo cells, K. H. Kingdon and H. E. Thomson—343
Pigment dispersions
Physics in the study of, F. A. Steele—101
Radiometers
Observation limit of radiometric measurements, C. Hawley Cartwright—211
Soils
Capillary conduction of water, L. A. Richards—318
Spark, electric
Time lag, John A. Tiedeman—354
Surface tension (see also **Capillarity**)
Capillary rise in sands, W. O. Smith, Paul D. Foote, P. F. Busang—18
Variation with pressure of saturation of gas-saturated petroleum, C. A. Swartz—245
Temperature
Distribution in solid bodies, J. B. Austin—75
Thermal expansion
Aluminum alloys, E. E. McCollough—334
Thermionics
Properties of barium films adsorbed on tungsten, Herbert Nelson—84
Thixotropy
Of litharge and glycerine, E. Karrer, P. Wasserman—393
Transmission lines
Charts for *E*, *I*, and *Z* of long lines, H. E. Hartig—380
Ultramicroscope
Adaptability to colloid systems, L. V. Foster—154
Visibility
Diffuse light and point sources, I. Langmuir, W. F. Westendorp—273
Wood
Methods of studying capillary structure; data on sapwood and heartwood, Alfred J. Stamm—116
X-rays
Tubes and their operation, W. D. Coolidge, L. E. Dempster, H. E. Tanis, Jr.—230